Reuse of *Cornus officinalis* Nutlet for Bioenergy

Xiaochen Yue,[a,#] Zhaolin Li,[a,#] Su Shiung Lam,[b] Wan-Xi Peng,[a,*] and Yifeng He [a,*]

As a traditional nourishing Chinese herbal medicine, *Cornus officinalis* Sieb. et Zucc. has a long history of application. At present, only the flesh of the fruit of *Cornus officinalis* is used as a medicine, which wastes a large quantity of ingredients in the nutlet. To improve the comprehensive utilization efficiency of the fruit's nutlet, which could be used when there is a shortage of the plant's fruit in the market, this study used Fourier transform-infrared spectroscopy (FT-IR), gas chromatography-mass spectrometry (GC-MS), thermogravimetric (TG) analysis, pyrolysis-gas chromatography-mass spectrometry (PY-GC-MS), and nuclear magnetic resonance (NMR) techniques to analyze the *Cornus officinalis* nutlet. The results showed that the active ingredients of *Cornus officinalis* nutlet have great medicinal value and could become a substitute for the fruit. After extracting the active ingredients, the residue can be used as a good biomass liquid fuel, providing reference for the future to replace fossil fuels. This study provides the scientific basis for the comprehensive utilization of high-quality resources for *Cornus officinalis*.

DOI: 10.15376/biores.17.4.6411-6444

Keywords: Cornus officinalis nutlet; NMR analysis; Py-GC-MS; TGA-DTG; Biofuel

*Contact information: a: School of Forestry, Henan Agricultural University, Zhengzhou 450002, China; b: Pyrolysis Technology Research Group, Institute of Tropical Aquaculture and Fisheries (AKUATROP), Universiti Malaysia Terengganu, 21030 Kuala Nerus, Terengganu, Malaysia;*Corresponding authors: heyifeng310@163.com; pengwanxi@163.com; #These authors equally contributed to this work as co-first authors.*

INTRODUCTION

Wood is an organic substance formed by natural growth. In addition to cellulose, hemicellulose, and lignin, it contains other minor components. Wood extract can be obtained with the use of ethanol, benzene, ethyl ether, acetone, dichloromethane, and other organic solvents. Wood extract contains more than 700 types of compounds, some of which can be used directly in dyes, preservatives, spices, activators, pesticides, and pharmaceuticals. However, few studies have researched the composition, content, and nature of wood extracts as biomass, which has not been given sufficient attention in the wood processing industry.

As a clean energy in the 21st century, there has been great interest in biomass energy because fossil resources are being depleted. Analyzing the composition of wood extracts increases the comprehensive understanding of the role and benefits that bioenergy can play. Tannins from bark can strengthen phenolic resin or urea-formaldehyde resin (Zhang *et al*. 2015). Wani *et al*. (1963) found that paclitaxel from mushroom extracts has an anti-cancer effect on leukemia, breast cancer, ovarian cancer, lung cancer, melanoma and colon cancer (Peng *et al*. 2017a; Ge *et al*. 2018). However, few studies have been conducted on the composition of the nutlet of *Cornus officinalis* using a variety of extraction methods.

Cornus officinalis Sieb. et Zucc. is a deciduous shrub or small tree of Cornaceae that produces clusters of fruits known as Asiatic cornelian cherries (Corni Fructus or Shu Zhu Yu). It is used as a food plant, and its mature fruit is also used in traditional Chinese medicine. The fruit is sour, astringent, tepid, and is used as a liver and kidney tonic. The active ingredient has antibacterial and diuretic properties, lowers blood pressure, decreases postprandial hyperglycemia, and stimulates the immune system and other physiological activity resin (Zhang *et al.* 2013; He *et al*. 2019). Immuno-pharmacological activity analysis of the various components isolated from the seed or nutlet of *Cornus officinalis* revealed some differences in their immunocompetence. Among them, both polysaccharides and glycosides have immunosuppressive effects. The effect of the monoterpenoid iridoid on the content of sICAM-1 and TNF-α in the model of vascular complications in diabetic rats may be related to its inhibitory effect on non-enzymatic glycation reaction (Gang *et al.* 2013). The nutlet extract of *Cornus officinalis* increases superoxide dismutase (SOD) blood activity in rats, inhibits free radical generation, and reduces malondialdehyde (MDA) levels (Tan *et al.* 2006). The annual output of *Cornus officinalis* fruit (COF) in China is more than 6000 tons every year, and in recent years, the inventory of COF is 3000 tons every year (Chen *et al.* 2012). The situation that the output of COF exceeds the sales is becoming increasingly obvious. In addition, the increase of manual picking costs has led to no one willing to manage the COF after it has become mature and abandoned, resulting in waste of *C. officinalis* resources. However, in view of the solution to this situation, the current research focuses on the use of *Cornus officinalis* nutlet as medicine instead of flesh to increase the application of COF. Little research on the application of *Cornus officinalis* nutlet as biofuel has been conducted. Therefore, it is more urgent to find ways to expand the application of *C. officinalis* and realize the maximum resource utilization of *C. officinalis*.

In this study, the components of *C. officinalis* nutlet (CON) from COF and its extracts were analyzed by Fourier transform-infrared spectroscopy (FT-IR), gas chromatography-mass spectrometry (GC-MS), thermogravimetric (TG) analysis, pyrolysis-gas chromatography-mass spectrometry (Py-GC-MS), and nuclear magnetic resonance (NMR) techniques, providing reference for the medical and industrial use of *C. officinalis* as a bioenergy source.

EXPERIMENTAL

Experimental Materials

The nutlets of *Cornus officinalis* were obtained from Xixia County Forest Farm, Nanyang City, Henan Province, China. The nutlets were dried, and it was confirmed that the pulp residues in the nutlets had been removed. The nutlets were extracted using four solvents (ethanol, methanol, ethanol/benzene (1:1), and ethanol/methanol (1:1)) and were named B1, B2, B3, and B4, as shown in Table 1. Then 20 g of CON powder was weighed for each, and organic solvent extraction was used to obtain the extracts. The amount of organic solvent was 300 mL, the extraction time was 4 hours, and the extraction temperature was 78 ℃ (B1), 64 ℃ (B2), 80 ℃ (B3), and 70 ℃ (B4). Finally, a rotary evaporator was used to concentrate the solution to 30 mL to obtain the extracts. The experimental process is shown in Fig. 1.

Table 1. Optimization of Experimental Program

No.	Solvent	M (g)
B1	C_2H_5OH	20.08
B2	CH_3OH	20.23
B3	C_6H_6/C_2H_5OH (1:1)	20.57
B4	CH_3OH/ C_2H_5OH (1:1)	20.31

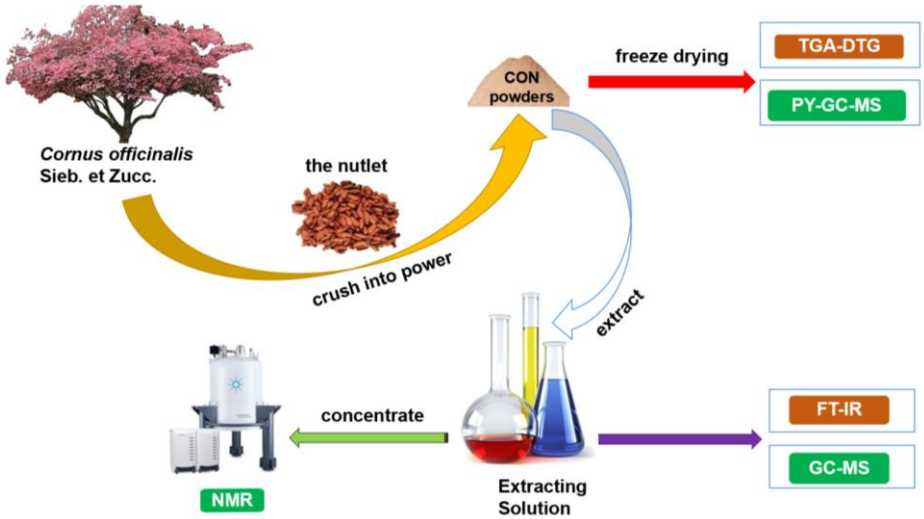

Fig. 1. Experimental flow chart

FT-IR

The samples were analyzed with a Fourier transform infrared (FT-IR) spectrophotometer (Shimadzu, Kyoto, Japan) using KBr discs containing 1.00% finely ground sample (Jiang *et al*. 2017; Peng *et al*. 2017a).

TGA-DTG

The CON powder was examined with a thermogravimetric analyzer (TGA Q50 V20.8 Build 34; TA Instruments, New Castle, DE, USA). The nitrogen release rate was 60 mL/min. The TG temperature program began at 30 ℃ temperature and increased to 300 ℃ at a rate of 5 ℃/min.

PY-GC-MS

The powder of CON was analyzed by thermal cracking-gas chromatography-mass spectrometry (CDS5000-Agilent7890B-5977A; Agilent Technologies, Santa Clara, CA, USA). The carrier gas used high purity helium, the pyrolysis temperature was 500 ℃, the heating rate was 20 ℃/ms, and the pyrolysis time was 15 s. The pyrolysis product transfer line and the injection valve temperature were set to 300 ℃. A capillary column HP-5MS was used (30 m × 0.25 mm × 0.25 μm), and shunt mode was used with a split ratio of 1:60 and shunt rate of 50 mL/min. The temperature of the GC program began at 40 ℃ for 2 min, increased to 120 ℃ at a rate of 5 ℃/min, and then increased to 200 ℃ at a rate of 10 ℃/min for 15 min.

GC-MS

The components of CON were analyzed by a gas chromatography-mass spectrometry (GC-MS) instrument (Agilent Technologies, Santa Clara, CA, USA). A quartz capillary column was used (30 mm×0.25 mm×0.25 μm) with the starting temperature at 50 ℃, and then the temperature was increased at a rate of 8 ℃/min up to 250 ℃ without retention, with a subsequent rate of 5 ℃/min to 300 ℃ without retention. The temperature of the inlet was 250 ℃, the column flow was 1.0 mL/min, the split ratio was 20:1, and the carrier gas used was high purity helium. For MS, the ionization mode was EI, the electron energy was 70 eV, the temperature of the ion source was 230 ℃, the temperature of the quadrupole was 150 ℃, and the starting point of the scan was 30 to 600 amu.

NMR

A Nuclear Magnetic Resonance Polarimeter (Agilent-400 MR; Agilent Technologies, Santa Clara, CA, USA) was used, and the solvent was Methanol-d4. One NMR probe was used to determine ^{1}H-NMR, ^{13}C-NMR, and 2D-NMR. The conditions were as follows: ^{1}H-NMR: duration 1.000 s, pulse 45 degrees, sample-and-hold time 2.556 s, pulse width 6410.3 Hz, and ^{1}H-NMR frequency 399.79 MHz. ^{13}C-NMR: duration 1.000 s, pulse 45 degrees, sample and hold time 1.311 s, pulse width 25000.0 Hz, ^{13}C-NMR frequency 100.53 MHz, hydrogen decoupling frequency 399.79 MHz, and power 38 dB. 2D-HSQC: duration 1.000 s, sample and hold time 0.150 s, two pulse widths 4807.7 Hz and 20105.6 Hz, frequency of 2D-HSQC 399.79 MHz, frequency of carbon decoupling 100.54 MHz, and power 38 dB (Lu *et al*. 2011; Albrecht-Schmitt 2012; Chow *et al*. 2014; Zabow *et al.* 2015; Wu *et al*. 2017).

RESULTS AND DISCUSSION

Chemical Composition of CON extracts

FT-IR analysis

Figure 2 shows the infrared contrast spectra of CON from the four extracts (Shenderova *et al.* 2011; Kaznowska *et al*. 2017; Koo *et al*. 2018). The absorption peaks in the infrared spectrum of 3400 cm^{-1} or more may be stretching vibrations or anti-telescopic vibrations of free hydroxyl groups in liquid water. The absorption peak is due to the intermolecular association near the broad peak at 3420 to 3300 cm^{-1}. Absorption peaks at 3030 cm^{-1} are formed by the stretching vibration of saturated C-H bonds. The absorption peak at 2925 cm^{-1} may be formed by antisymmetric stretching of the CH_2 group. The absorption peak at 2380 to 2300 cm^{-1} is formed by the antisymmetric expansion of CO_2. The absorption peak at 1750 to 1650 cm^{-1} is due to the C=O double bond stretching vibration. The absorption peak at 1450 cm^{-1} is due to the CH_3 asymmetric corner vibration formation. The absorption peak at 1200 cm^{-1} is the C-O-C antiscathetic stretching of the ester species. The absorption peak at 1100 cm^{-1} is due to the symmetric and antisymmetric C-O-C stretching of esters and ethers, respectively. The absorption peak at 940 cm^{-1} may be formed by out-of-plane bending of COH. The absorption peaks of cellulose (at 2950 cm^{-1}), hemicellulose (1730 cm^{-1}), and lignin (1739 cm^{-1}, 1630 cm^{-1}, and 878 cm^{-1}) were slightly decreased in the chemical composition tested, indicating that hydrolysis occurred in part of it (Xu *et al.* 2013, Hu *et al.* 2014; Ge *et al.* 2018). The absorption peaks of the extracts are mainly concentrated in the bands of 3700 to 3000 cm^{-1}, 3000 to 2850 cm^{-1}, and

1690 to 870 cm^{-1}. The main chemical components were esters, aldehydes, ethers, fatty acids, hydrocarbons, and aromatics. In addition, the characteristic absorption peaks decreased, indicating partial extraction of esters, alcohols, ethers, fatty acids, hydrocarbons, and aromatics (Bassilakis *et al.* 2001; Peng *et al.* 2017b; Jiang *et al.* 2018).

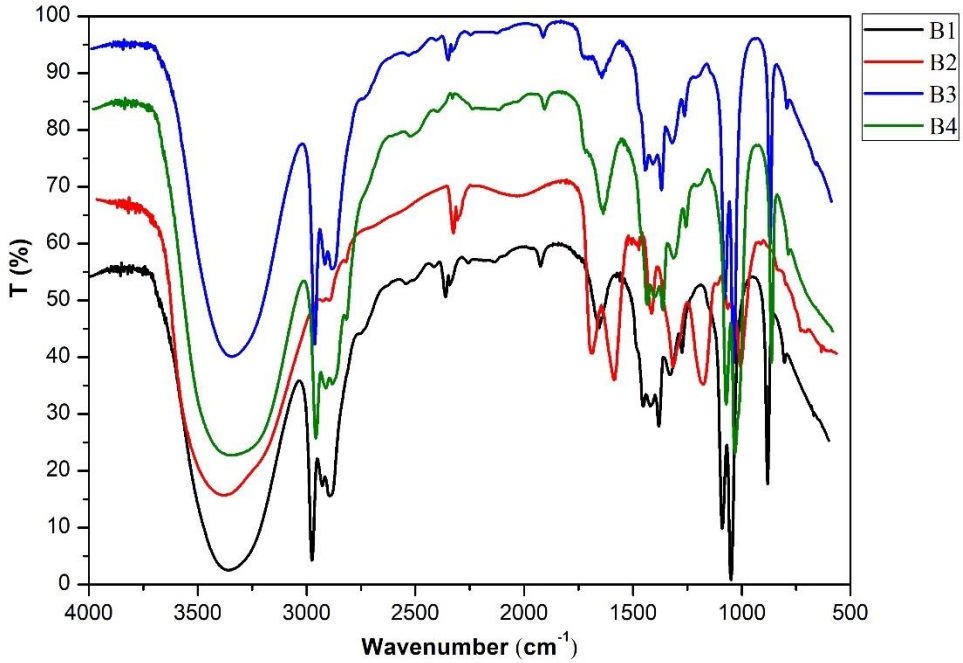

Fig. 2. FT-IR spectra of samples B1, B2, B3, and B4

GC-MS analysis

The total ion chromatograms of four types of extractives analyzed by GC-MS are shown in Figs. 3 through 6. The spectrum of each peak was retrieved using a computer and the wiley7n.1 standard spectrum. The peak area normalization method was used to calculate the content of each component, and specific results are shown in Tables S1 through S4.

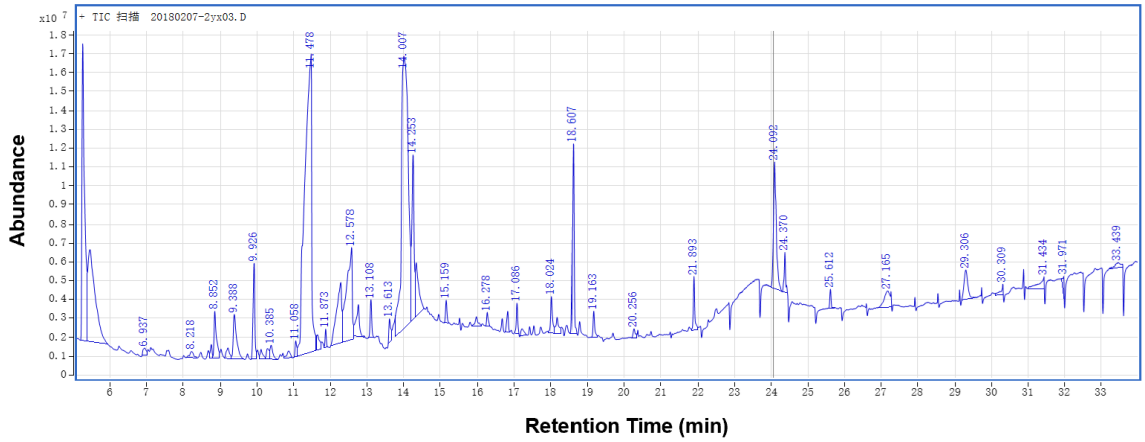

Fig. 3. Total ion chromatograms of ethanol extract from CON

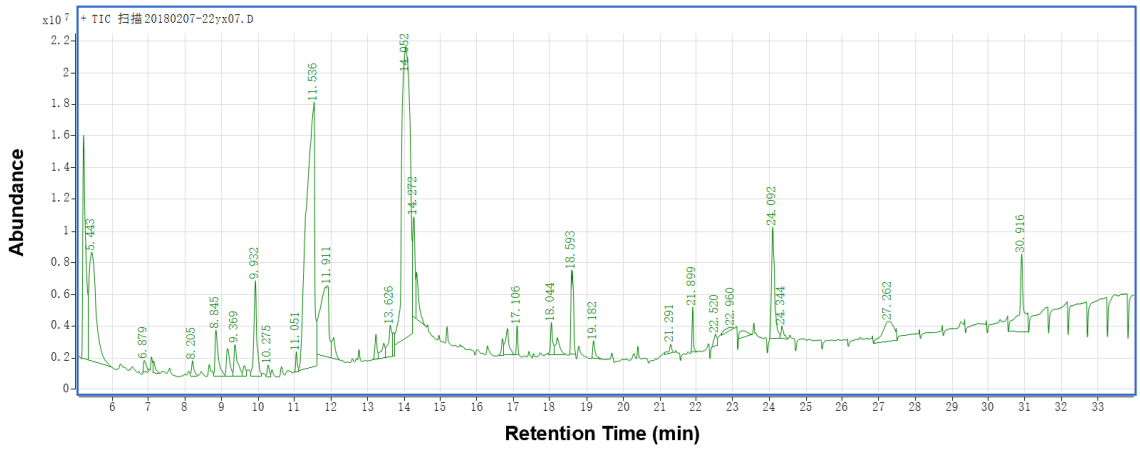

Fig. 4. Total ion chromatograms of a methanol extract of CON

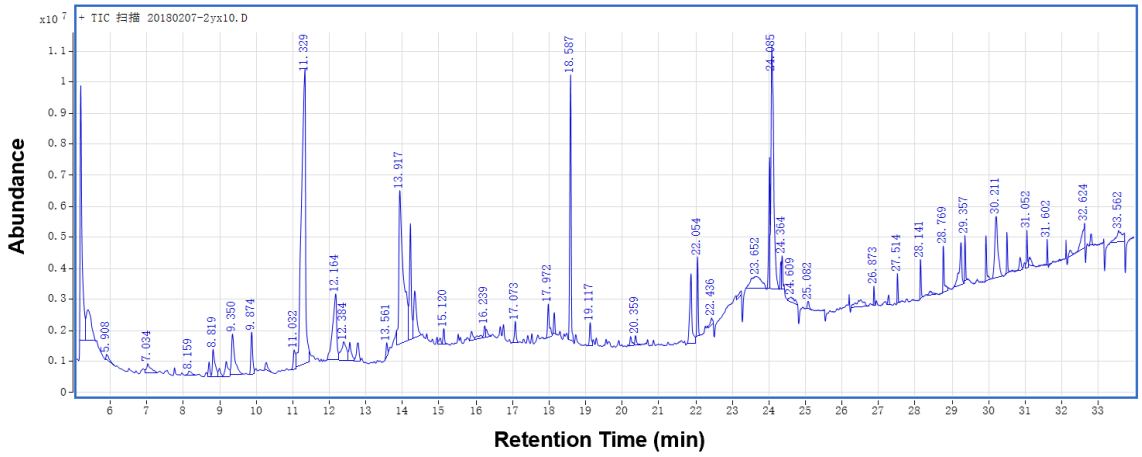

Fig. 5. Total ion chromatograms of ethanol/benzene extract from CON

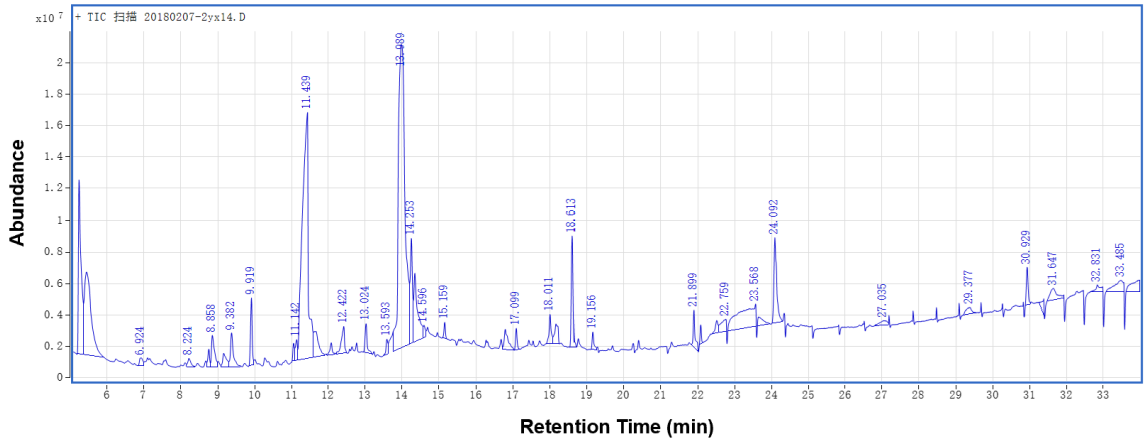

Fig. 6. Total ion chromatograms of ethanol/methanol extract from CON

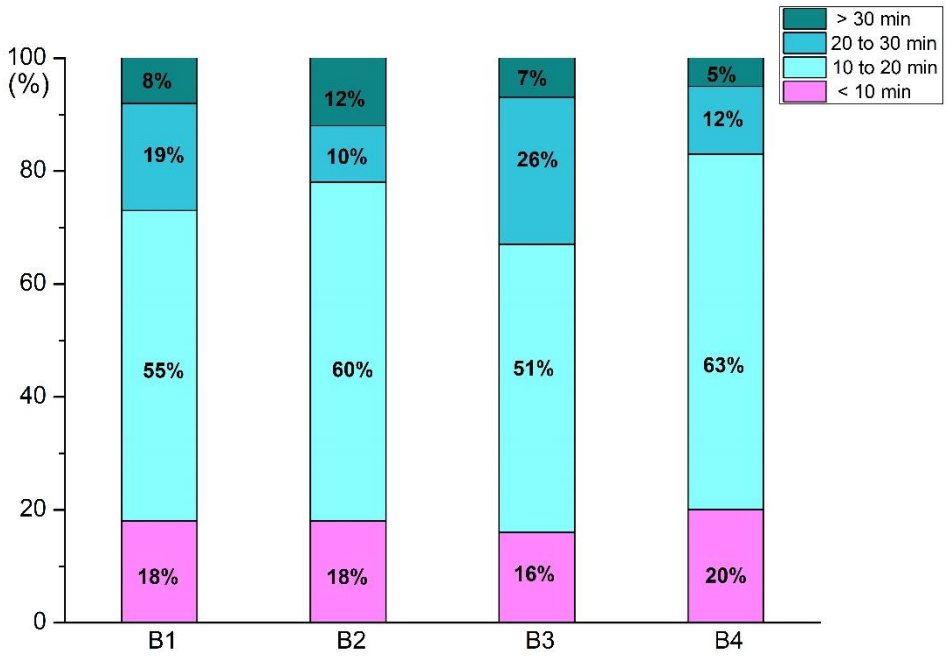

Fig. 7. Distribution of samples B1, B2, B3, and B4 after GC-MS analysis

According to the results of GC-MS analysis, 93 peaks were detected in B1, and 93 chemical constituents were identified. The results show that the content of more substances were as follows: 3-Furaldehyde (9.21%), Maleic anhydride (4.44%), 4H-Pyran-4-one,2,3-dihydro-3,5-dihydroxy-6-methyl- (1.46%), 5-Hydroxymethylfurfural (16.48%), Malic acid (7.08%), 4-Ethylbiphenyl (2.93%), 1,2,3-Benzenetriol (16.61%), Vanillin (1.82%), Spiro[4.5]decan-7-one, 1,8-dimethyl-8,9-epoxy-4-isopropyl- (2.58%), 9,12-Octadecadienoic acid (Z,Z)- (2.30 %), Ethylamine, N,N-diheptyl-2-(2-thiophenyl)- (1.88 %), octamethyl-Cyclotetrasiloxane, (1.37 %), and 4-butoxy-1,1'-Biphenyl (1.53 %).

According to the results of the GC-MS analysis, 65 peaks were detected in B2, and 65 chemical constituents were identified. The results show that the content of more substances were as follows: 3-Furaldehyde(7.29%), Maleic anhydride(5.25%), 4H-Pyran-4-one, 2,3-dihydro-3,5-dihydroxy-6-methyl-(1.95%), 5-Hydroxymethylfurfural(17.34%), Malic acid(4.29%), 4-Ethylbiphenyl(5.25%), 1,2,3-Benzenetriol(23.46%), Vanillin (1.25%),Spiro[4.5]decan-7-one, 1,8-dimethyl-8,9-epoxy-4-isopropyl- (1.58%), 1H-Benzo[d,E]phthalazine, 6-methoxy-1,3-dimethyl- (2.48%), 9,12-Octadecadienoic acid (Z,Z)- (2.21%), 6H-Dibenzo[b,d]pyran-6-one, 7,9-dihydroxy-3-methoxy-1-methyl- (1.16%), 4-Methyl-2,4-bis(p-hydroxyphenyl)pent-1-ene, 2TMS derivative (1.77%), 4-Methyl-2,4-bis(p-hydroxyphenyl)pent-1-ene and 2TMS derivative(1.54%).

According to the results of GC-MS analysis, 66 peaks were detected in B3, and 59 chemical constituents were identified. The results show that the content of more substances were as follows: Furfural (6.88%), 1H-Imidazole, 1,2-dimethyl- (2.37%), Levoglucosenone (2%), 5-Hydroxymethylfurfural (18%), Malic acid (3.92%), 1,2-Cyclobutanedicarboxylic acid, trans- (2.16%), 1,2,3-Benzenetriol (10.13%), Benzaldehyde, 3-hydroxy-4-methoxy- (3.31%), 2-(4'-Methoxymethylbiphenyl-4-yl)propan-2-ol (1.97%), 2-Acetoxy-3,3-dimethyl-2-(3-oxo-but-1-enyl)-cyclobutanecarboxylic acid, methyl ester (5.34%), N-2,4-Dnp-L-arginine (2.30%), 9,12-

Octadecadienoic acid (Z,Z)-(11.92%) and Heptasiloxane, 1,1,3,3,5,5,7,7,9,9,11,11,13,13-tetradecamethyl- (3.76%).

According to the results of GC-MS analysis, 43 peaks were detected in B4, and 39 chemical constituents were identified. The results show that the content of more substances were as follows:3-Furaldehyde (6.16%), Maleic anhydride (7.45%), 4H-Pyran-4-one, 2,3-dihydro-3,5-dihydroxy-6-methyl- (1.44%), 5-Hydroxymethylfurfural (18.87%), Thiophene, 2-propyl-(1.66%),1,2,3-Benzenetriol (32.63%), 2-Acetoxy-3,3-dimethyl-2-(3-oxo-but-1-enyl)-cyclobutanecarboxylic acid, methyl ester (2.39%),2,5-dimethoxy-4-ethylthio-benzaldehyde (6.42%), 9,12-Octadecadienoic acid (Z,Z)- (3.06%) and Octasiloxane, 1,1,3,3,5,5,7,7,9,9,11,11,13,13,15,15-hexadecamethyl- (1.54%).

Figure 7 shows that there were different distributions of the retention time of different components from the hawthorn kernel. For B1 sample, 18%, 55%, 19%, and 8% sample retention times were less than 10, 20, and 30 min, and greater than 30 min, respectively. For B2 sample, 18%, 60%, 10%, and 12% of the sample components had retention times less than 10, 20, and 30 min, and retention times greater than 30 min, respectively. For B3 sample, 16%, 51%, 26%, and 7% sample components retained retention times of less than 10, 20, and 30 min and greater than 30 min, respectively. For B4 sample, the 20%, 63%, 12%, and 5% sample retention times were less than 10, 20, and 30 min, and greater than 30 min, respectively (de Jong *et al.* 2018; Wan-Ibrahim *et al.* 2018; Wang *et al.* 2018).

Analysis of NMR spectra

The ^{1}H-NMR spectrum is the most widely used nuclear magnetic resonance spectrum. As the hydrogen core has a large magnetic spin ratio γ, its magnetic properties are strong, the detection sensitivity is high, and the signal is easy to observe (Lanza *et al.* 2010). There are a large number of hydrogen atoms in different chemical environments of organic compounds, and therefore, the ^{1}H-NMR spectrum can provide important structural information for many organic compounds (Fig. 8) (Feigenson and Meers 1980; Martin *et al.* 2008; Maulidiani *et al.* 2018; Pinto *et al.* 2018). The chemical shifts of protons are mainly distributed in the alkane compounds saturated at δ 0.6 to δ 1.6. At other locations, the peak of δ 3.34 should be the CD_3OD solvent peak. The first proton occurs at a δ value of approximately 1.15 pm, and the chemical shift value at this position should be the alkane proton(-C-C-H). The first proton moves slightly to the right and appears at a delta value of approximately 1.3 ppm. Near the delta value of 3.3 to 3.6 ppm, the solvent peak of CH_3OH is predominant. Proton chemical shifts on carbon atoms directly attached to the halogen also occur at this position. The chemical shifts of the protons on α-C in the vicinity of the carbonyl or cyanide groups are 2 to 3 μm with an anisotropic effect on C=C and the sp2 hybridization of olefinic carbons. The chemical shift of olefinic compounds is within 4.5-6 μm. When change occurs, coupled with aryl, the value of δ will increase; the peak is most obvious at δ5.3 and δ7.0. The chemical shift of α-H in the hydrogen atom of the ether molecule is approximately 3.5 ppm. The δ value of the hydroxyl proton is approximately 4 to 8 ppm. The chemical shift of the aromatic compound is in the range of 6.3 to 8.5, and the value of the heterocyclic aromatic proton is within the range of 6.0 to 9.0. Based on the peaks of the specific chemical shifts shown by the ^{1}H-NMR spectrum, additional compounds from CON can be roughly determined.

Carbon makes up the skeleton of organic molecules. The importance of ^{13}C NMR analysis to chemical research is clearly recognized. The chemical shift of ^{1}H NMR is usually in the range of 0 to 15 ppm, while the usual range of ^{13}C NMR is 0 to 300 ppm,

which is approximately 20 times that of ^{1}H (De Feyter *et al.* 2018; Lusk and Gullion 2018; Tang *et al.* 2018). In the ^{1}H NMR, it is not directly observed that the absorption signal of hydrogen groups such as C=O, C=C, and C=N can be clear, given their characteristic absorption peak by ^{13}C NMR. Figure 9 is a study of the structural change of a sample using ^{13}C-NMR spectroscopy. Between 10 and 50 ppm, mainly chemical bond shifts of saturated alkanes occur. As can be seen from the figure, the first proton appears at a δ value of approximately 18 ppm. The chemical shift value at this position should be the alkane proton-(CH_2)-CH_3. The second proton shifts back, showing a δ value of 40 ppm. Where possible, the chemical bond at this location should be an alkane containing the N element. For carbohydrate polymer carbon, all important signals are generally distributed in the 50-110 ppm region (Xue *et al.* 2014). The chemical shift value of the alkyne alkynyl carbon should be near 69 ppm and 78 ppm, and the chemical bonds present are predominantly -C=C-bonds. The chemical shift value of the olefinic carbon is between 100 and 120 ppm. The chemical bonds at the peaks of 98 ppm and 110 ppm are -HC-CH-. The chemical shift values of the aromatic ring carbons and heteroaromatic ring carbons are generally in the range of 120 to 160 ppm, and peaks tend to appear in lower fields. A peak appeared at 145 ppm, which may be the chemical shift values of benzene and its derivatives. Among the hydroxy compounds, because the electron density of the π-bonds in C=O is small, the chemical shift value tends to be lower in the field, and the δ value generally appears between 160 and 220 ppm. The peak appears at 172 ppm and 176 ppm and is probably a hydroxycarbon compound (Sharma and Rajarathnam 2000; Cimino *et al.* 2004; Xie *et al.* 2017; Gurjar and Kaur 2018).

2D-HSQC is one of the most common two-dimensional NMR spectra. It provides information on ^{1}H nucleus and ^{13}C nucleus single bonds and is of great significance for structural analysis (Moniz *et al.* 2018; Xiao *et al.* 2018; Yao *et al.* 2018). It is also available in ^{1}H and ^{13}C-NMR spectra. The resolution of overlapping signals reveals the link between these two aromatic units (Shupe *et al.* 2012; Fu *et al.* 2017; Fakeeha *et al.* 2018; Khan *et al.* 2018). To obtain further information on the structural characterization of methanol/ethanol samples, 2D-HSQC NMR analysis was performed. The aliphatic region (δC/δH 10–40/0.5–2.5), side chain (δC/δH 50–95/2.5–6.0), and the aromatic (δC/δH 95–150/5.5–8.0) region of the HSQC spectra of the sample are shown in Figure 10. Additionally, δC/δH 110/6.97, δC/δH 120/6.8, δC /δH 114/6.7, δC/δH 104/6.68, δC/δH 72/4.82, and δC/δH 86/4.19 illustrate the interconnected hydrogen and carbon. As shown by 2D-HSQC NMR, δC/δH 15-45/0.2–1.5 are a hydrocarbon-saturated hydrocarbon connection. δC/δH 55-75/4.5–6.5,1.7-3.5 are mainly the carbon spectra of some alkynes and some of the olefins. δC/δH 110-140/6.3–8.3, 4.5–6.5 are predominantly aromatic and olefinic carbons. δC/δH 60-80/3.1–4 are alcohols, ethers, phenols, and other oxygen-containing compounds.

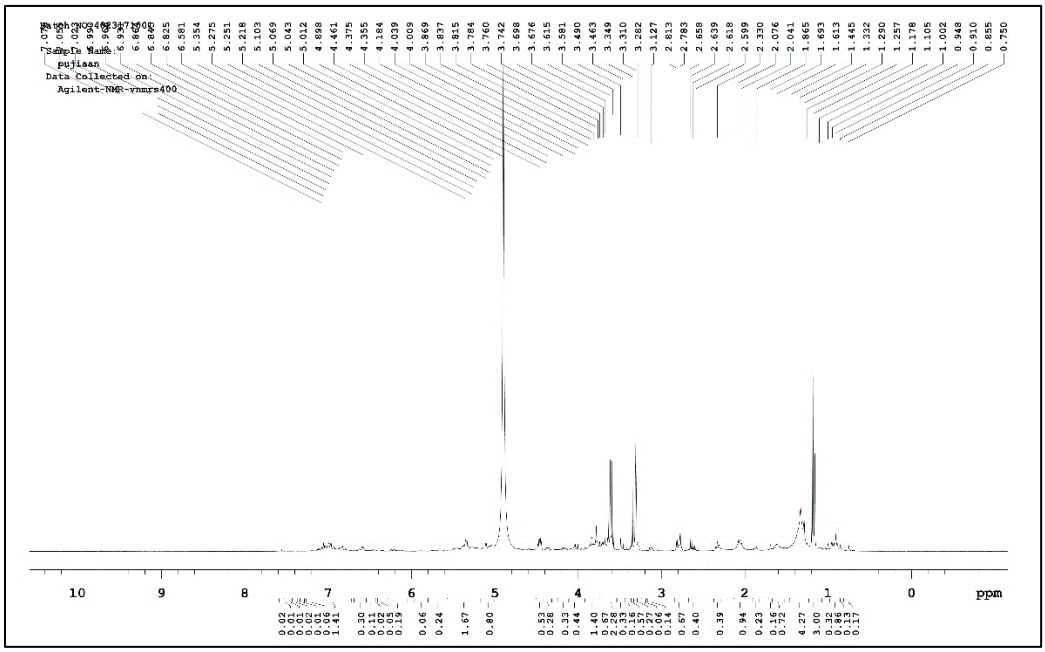

Fig. 8. ^{1}H-NMR spectra of the sample

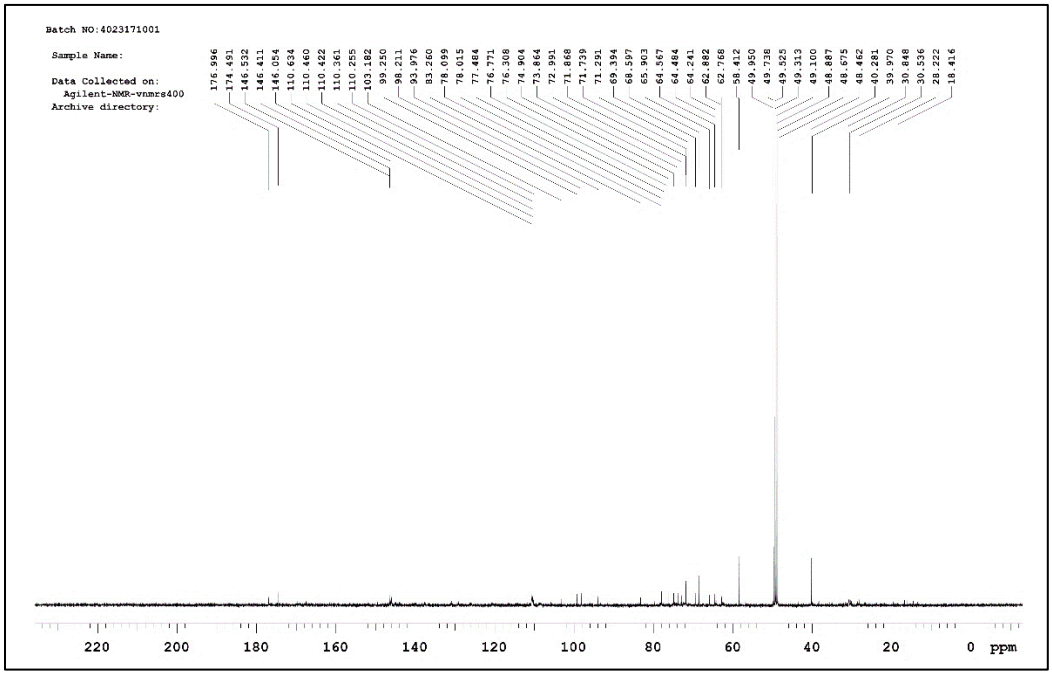

Fig. 9. ^{13}C-NMRspectra of the sample

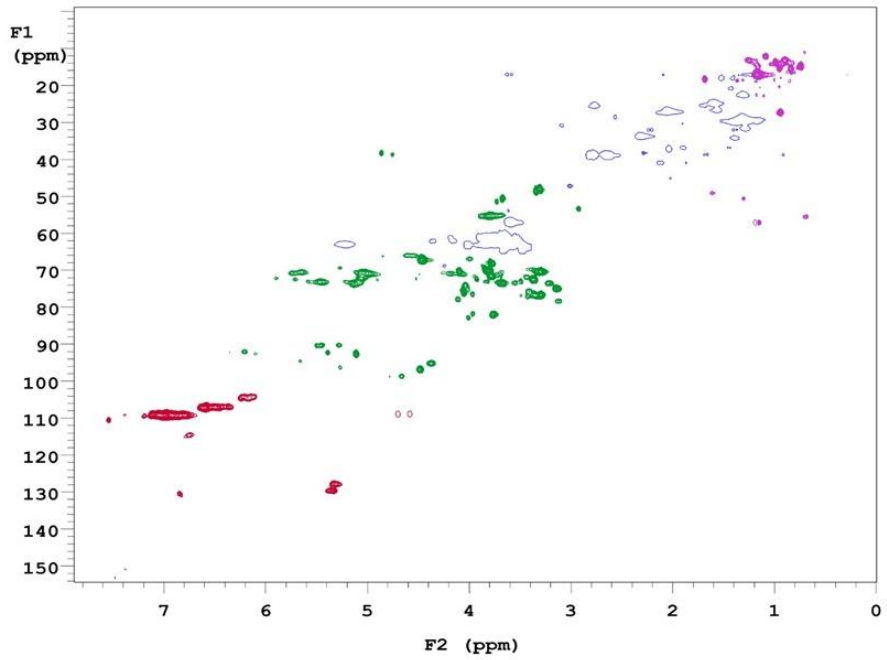

Fig. 10. 2D-HSQC NMR spectra of CON

Medicinal properties

The compounds identified in Tables S2 to S5 in the Appendix are also classified as esters, acids, phenols, tannins, iridoids, soaps, ketones, and glycosides. Among them, CON exhibits immunostimulant activity, and glycosides exhibit immunosuppressive and immunomodulatory effects. The iridoid glycosidesin from CON can reduce the serum levels of ICAM-1 and TNF-α in the vascular complication model of diabetic rats, thus resulting in the hypoglycemic effect of total terpenes in CON (Hong *et al.* 2003; Han *et al.* 2006; Hu *et al.* 2009). In addition, iridoid glycosides may inhibit thrombosis by changing the state of hypercoagulability of the blood and provide a good experimental basis for the prevention and treatment of thrombotic diseases. CON contains polyphenolic compounds, one of which is an ortho-phenolic hydroxyl that can be easily oxidized, and the active oxygen and other free radicals have a strong ability to be captured, making it a strong antioxidant and scavenger of free radicals. Maleic anhydride is an important basic raw material for unsaturated organic acid anhydride. It is used in pesticide production to synthesize organic phosphorus pesticides. Maleic anhydride is also used to produce unsaturated polyester resin, papermaking auxiliary, coatings, and pharmaceutical industry (Popadyuk *et al.* 2013). 5-Hydroxymethylfural (5-HMF) is an important furan compound. Because of its excellent chemical properties, it is widely used in medicine, chemistry, energy and other fields. Its derivatives have significant application prospects in fine chemicals, medicine, degradable plastics and other fields (Atanda *et al.* 2016). These active ingredients from CON are the same or similar to those reported in the COF (Gang *et al.* 2013; Zhang *et al.* 2013; He *et al.* 2019).

Behavior during Combustion of CONs

TGA and DTG analysis

The thermal stability of CON is largely responsible for its excellent flame-retardant properties, but it also determines the broad application prospects (Salasinska *et al.* 2020).

Thermal stability analysis is an effective method to evaluate the flame retardancy and industrial applications of CON (Xie *et al*. 2011; Renneckar *et al.* 2004). Figure 11 shows the TGA curve and DTG curves of CON. According to Fig. 11, T5wt.% and T10wt.% are at 157 ℃ and 234 ℃, respectively. There are three stages in the process of weight loss. The first stage is 20 to 106 ℃, when small molecules with low moisture content and boiling point undergo evaporation. The weight loss during this stage is 4.6%. The second stage is 106 to 200 ℃. As long as the material component is slightly cracked, the weight loss is only 3%. The third stage is 200 to 300 ℃. At this decomposition stage, the organic matter of the components has undergone severe cracking with increasing temperature and the burning of other components. The content of the material has been reduced from 93.5% to 73.9%. The DTG curve at this stage is constantly increasing, indicating that the rate of material weight loss is also increasing (Dochia *et al.* 2018; Guo *et al.* 2019).

The three phases showed different properties and phenomena, with different kinetic parameters and reaction mechanisms, with a final residual mass of 73.9% (Rukthong *et al.* 2015; Liu *et al.* 2018; Lou *et al.* 2018). Between 20 and 250 ℃, CON showed a thermal weight of approximately 13 wt.%, and the weight loss was low, especially before 200 ℃. The weight loss was only 6.5%, indicating that CON had good thermal stability. Throughout the TG experimental tests, CON demonstrated good thermal stability within 200 ℃, indicating that it has excellent processing properties, and good prospects for research and industrial use.

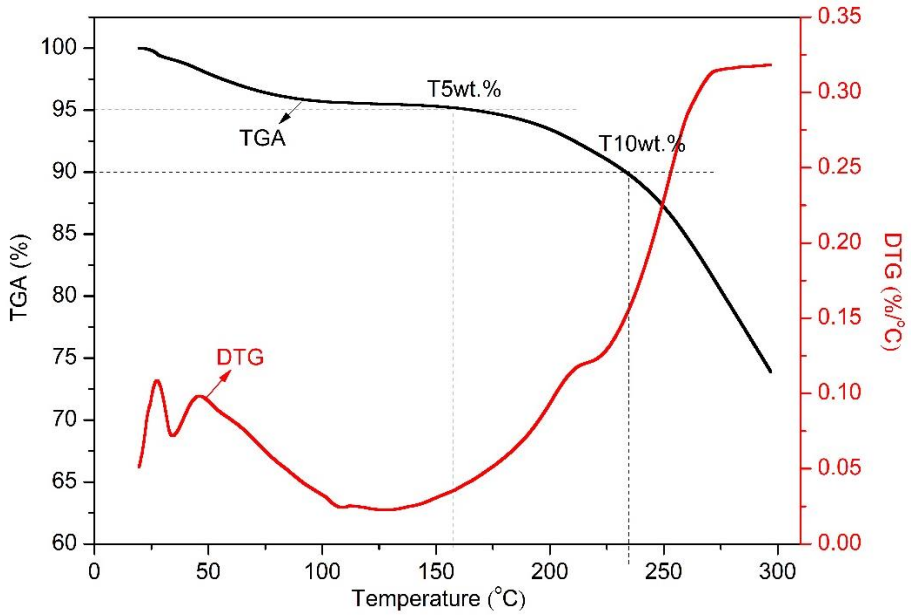

Fig. 11. TGA and DTG thermal curves for CON

Py-GC-MS analysis

The total ion chromatograms of CON by Py-GC-MS are shown in Fig. 12 and the relative content of each component has been counted by area normalization (Lan and Peng 2012; Peng *et al.* 2012). The MS data was analyzed using the NIST standard MS map and publicly published books and articles, and then identifying each component. The analytical results are listed in Table S5.

According to the results of the Py-GC-MS analysis, 241 peaks were detected in Table 6, and 241 chemical constituents were identified. The results show that the content

of more substances are as follows: 4-methyl-2-Hexanamine (2.82%), Glycidol (1.33%), Formic acid (1.13%), Acetic acid (8.72%), Furfural (2.78%), 1,2-Cyclopentanedione (1.06%), 2,2-diethyl-3-methyl-Oxazolidine (1.02%), 2-Methyliminoperhydro-1,3-oxazine (1.07%), 2-methoxy-Phenol (2.21%), Creosol (1.95%), Catechol (1.67%), 5-Hydroxymethylfurfural (2.07%), 2-Methoxy-4-vinylphenol (2.55%), 2,6-dimethoxy-Phenol (1.87%), 1,2,3-Benzenetriol (1.29%), Vanillin (1.81%), 3,5-Dimethoxy-4-hydroxytoluene (1.55%), trans-Isoeugenol (1.52%), 1-(4-hydroxy-3-methoxyphenyl)-2-Propanone (1.11%), (E)-Stilbene (3.27%), D-Allose (1.95%), 1,6-anhydro-.beta.-D-Glucopyranose (1.67%), (E)-2,6-Dimethoxy-4-(prop-1-en-1-yl)phenol (1.12%), and *n*-Hexadecanoic acid (1.31%).

As shown in Fig. 13, there was a different distribution of retention times for the different components of CON. The retention times of 22%, 18%, 48%, and 12% for the sample component content were less than 10, 20, and 30 min and greater than 30 min, respectively. The molecular weight increases occurred in sample retention times greater than 30 min, 10-20 min, less than 10 min, and 20-30 min, with a higher molecular weight content than the other retention times in the 20-30 min retention period (Toraman *et al.* 2017; Dziwiński *et al.* 2018; Fang *et al.* 2018; Yu *et al.* 2018).

Glycidol obtained by pyrolysis contains epoxy group and hydroxyl group. It has active chemical properties and can carry out many ring opening reactions. Glycidol is hydrolyzed to generate glycerol, and propylene glycol is generated through catalytic hydrogenation, which is condensed with alcohols to generate glycerol ether (Bakhiya *et al.* 2011). It is often used in surface coatings, chemical synthesis, production of fungicides and so on. Another pyrolysis product, Vanillin, is the first essence synthesized by human beings. As an important edible flavor, Vanillin is used in almost all flavor types and is widely used in the food industry. In addition, the application of Vanillin in the medical field has been continuously expanded in recent years and has become the most potential field for Vanillin application (Abraham *et al.* 1991; Fitzgerald *et al.* 2004). The content of organic and inorganic substances in biomass combustion process determines whether it can be used as a good biofuel. The higher the inorganic content in the combustion process, the more unfavorable the element occurrence mode (chloride, sulfate, carbonate, oxalate, nitrate and some hydroxide, phosphate) (Vassilev and Vassileva 2016). The application and processing of these biofuels will lead to environmentally challenging thermochemical conversion. However, the main components of the detected from CON were esters, acids, phenols, anthraquinones and ketones, and the content of inorganic salts was relatively low (Table S5). By analyzing the main functions and functions of different compounds, CON can be more effectively and fully utilized.

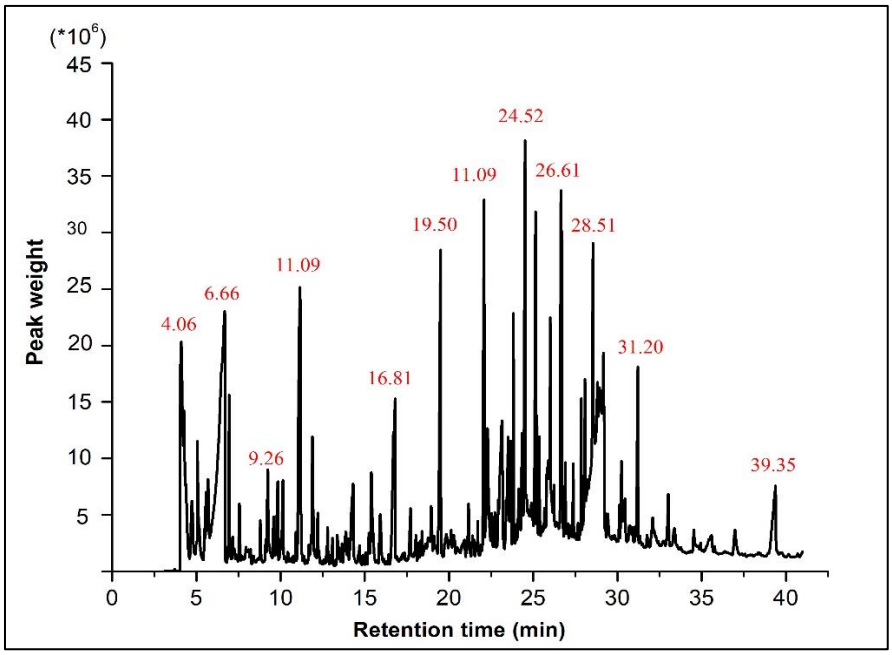

Fig. 12. Total ion chromatograms of CON by Py-GC-MS

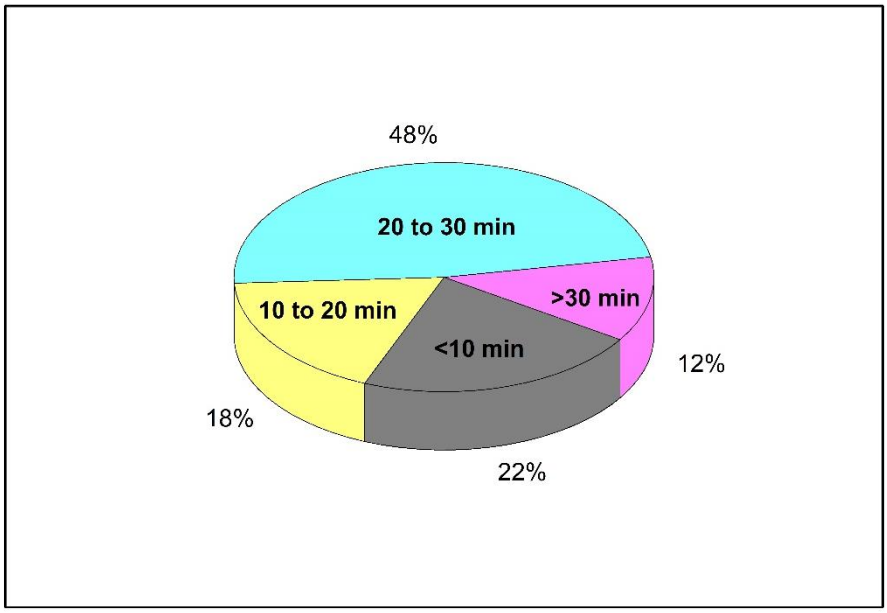

Fig. 13. Distribution characteristic of CON by Py-GC-MS

CONCLUSIONS

1. The absorbance peaks of the extract of *Cornus officinalis* nutshells (CONs) were concentrated in the 3700 to 3000 cm^{-1}, 3000 to 2850 cm^{-1}, and 1690 to 870 cm^{-1} bands. The decrease in the characteristic absorption peak indicates that the esters, alcohols, ethers, fatty acids, hydrocarbons, and aromatic compounds had been partially extracted. By the identification using gas chromatography-mass spectrometry (GC-MS) tests,

more than 60 kinds of chemical active ingredients were detected, which can play a certain role in immune regulation, hypoglycemia, inhibition of thrombosis formation, and anti-oxidation.

2. Through the research and analysis of the extract of CON, it was determined that the seed also has the same important medical value as the pulp, and has great application prospects in medicine and food.
3. In addition, in the CON extracts, many organic substances were the same or homologous to biomass oil, and the residue after the active ingredient is extracted can be used as a biomass liquid fuel. It may be possible to use it in place of fossil energy sources. After the above analysis, we want to provide the scientific basis for CON to become a high-quality resource.

ACKNOWLEDGMENTS

This study was supported by the Program for Innovative Research Team (in Science and Technology) in University of Henan Province (No. 21IRTSTHN020), and Central Plain Scholar Funding Project of Henan Province (No. 212101510005).

Declaration of Competing Interest

The authors declare that they have no known competing financial interests or personal relationships.

REFERENCES CITED

Abraham, D. J., Mehanna, A. S., Wireko, F. C., Whitney, J., and Orringer, E. P. (1991). "Vanillin, a potential agent for the treatment of sickle cell anemia," *Blood* 77(6), 1334-1341. DOI: 10.1182/blood.V77.6.1334.1334

Albrecht-Schmitt, T. E. (2012). "NMR tools for determining the structure of plutonium materials," *Science* 336(6083), 811-812. DOI: 10.1126/science.1222927

Atanda, L., Konarova, M., Ma, Q., Mukundan, S., Shrotri, A., and Beltramini, J. (2016). "High yield conversion of cellulosic biomass into 5-hydroxymethylfurfural and a study of the reaction kinetics of cellulose to HMF conversion in a biphasic system," *Catalysis Science & Technology* 6(16), 6257-6266. DOI: 10.1039/c6cy00820h

Bakhiya, N., Abraham, K., Gürtler, R., Appel, K. E., and Lampen, A., (2011). "Toxicological assessment of 3-chloropropane-1,2-diol and glycidol fatty acid esters in food," *Molecular Nutrition & Food Research* 55(4), 509-521. DOI: 10.1002/mnfr.201000550

Bassilakis, R., Carangelo, R. M., and Wójtowicz, M. A. (2001). "TG-FTIR analysis of biomass pyrolysis," *Fuel* 80(12), 1765-1786. DOI: 10.1016/S0016-2361(01)00061-8

Chen, Y. H., Feng, J. C., Zheng, X. B., Li, J. D., Wu, Y. X., Bi, H. T. (2012). "Development and prospects of researches on Cornus officinalis," *Nonwood Forest Research* 30(1), 143-150. DOI: 10.3969/j.issn.1003-8981.2012.01.029

Chow, W. Y., Rajan, R Muller, K. H., Reid, D. G., Skepper, J. N., Wong, W. C., Brooks, R. A., Green, M., Bihan, D., Farndale, R. W., Slatter, D. A., Shanahan, C. M., and Duer, M. J. (2014). "NMR spectroscopy of native and *in vitro* tissues implicates

polyADP ribose in biomineralization," *Science* 344(6185), 742-746. DOI: 10.1126/science.1248167

Cimino, P., Gomez-Paloma, L., Duca, D., Riccio, R., and Bifulco, G. (2004). "Comparison of different theory models and basis sets in the calculation of ^{13}C NMR chemical shifts of natural products," *Magnetic Resonance in Chemistry* 42, S26-S33. DOI: 10.1002/mrc.1410

De Feyter, H. M., Herzog, R. I., Steensma, B. R., Klomp, D. W. J., Brown, P. B., Mason, G. F., Rothman, D. L., and de Graaf, R. A. (2018). "Selective proton-observed, carbon-edited (selPOCE) MRS method for measurement of glutamate and glutamine, C-13-labeling in the human frontal cortex," *Magnetic Resonance in Medicine* 80(1), 11-20. DOI: 10.1002/mrm.27003

de Jong, W. H. A., Buitenwerf, E., Pranger, A. T., Riphagen, I. J., Wolffenbuttel, B. H. R., Kerstens, M. N., and Kema, I. P. (2018). "Determination of reference intervals for urinary steroid profiling using a newly validated GC-MS/MS method," *Clinical Chemistry and Laboratory Medicine* 56(1), 103-112. DOI: 10.1515/cclm-2016-1072

Dochia, M., Chambre, D., Gavrilas, S., and Moisa, C. (2018). "Characterization of the complexing agents' influence on bioscouring cotton fabrics by FT-IR and TG/DTG/DTA analysis," *Journal of Thermal Analysis and Calorimetry* 132(3), 1489-1498. DOI: 10.1007/s10973-018-7089-y

Dziwiński, E. J., Ilowska, J., and Gniady, J. (2018). "Py-GC/MS analyses of poly(ethylene terephthalate) film without and with the presence of tetramethyl-ammonium acetate reagent. Comparative study," *Polymer Testing* 65, 111-115. DOI: 10.1016/j.polymertesting.2017.11.009

Fakeeha, A. H., Ibrahim, A. A., Khan, W. U., Seshan, K., Al Otaibi, R. L., Al-Fatesh, A. S. (2018). "Hydrogen production via catalytic methane decomposition over alumina supported iron catalyst," *Arabian Journal of Chemistry* 11(3), 405-414. DOI: 10.1016/j.arabjc.2016.06.012

Fang, S. W., Yu, Z. S., Ma, X. Q., Lin, Y., Chen, L., and Liao, Y. F. (2018). "Analysis of catalytic pyrolysis of municipal solid waste and paper sludge using TG-FTIR, Py-GC/MS and DAEM (distributed activation energy model)," *Energy* 143, 517-532. DOI: 10.1016/j.energy.2017.11.038

Feigenson, G. W., and Meers, P. R. (1980). "^{1}H NMR study of valinomycin conformation in a phospholipid bilayer," *Nature* 283(5744), 313-314. DOI: 10.1038/283313a0

Fitzgerald, D. J., Stratford, M, Gasson, M. J., Ueckert, J., and Narbad, A. (2004). "Mode of antimicrobial action of vanillin against *Escherichia coli*, *Lactobacillus plantarum*, and *Listeria innocua*," *Journal of Applied Microbiology* 97(1), 104-113. DOI: 10.1111/j.1365-2672.2004.02275.x

Fu, H. L., and Liu, X. J. (2017). "Research on the phenomenon of Chinese residents' spiritual contagion for the reuse of recycled water based on SC-IAT," *Water* 9(11), DOI: 10.3390/w9110846

Gang, C., Hao, C., Cai, B., and Tu, S. (2013). "Effect of 5-hydroxymethylfurfural derived from processed *Cornus officinalis* on the prevention of high glucose-induced oxidative stress in human umbilical vein endothelial cells and its mechanism," *Food Chemistry* 140(1-2), 273-279. DOI: 10.1016/j.foodchem.2012.11.143

Ge, S. B., Gu, H. P., Ma, J. J., Yang, H. Q., Jiang, S. C., Liu, Z. L., and Peng, W. X. (2018). "Potential use of different kinds of carbon in production of decayed wood

plastic composite," *Arabian Journal of Chemistry* 11(6), 838-843. DOI: 10.1016/j.arabjc.2017.12.026

Gurjar, D. S., and Kaur, R. (2018). "Impact of wastewater irrigations and planting methods on leaf firing, colour, quality and traffic tolerance of turfgrass," *Journal of Environmental Biology* 39(1), 117-121. DOI: 10.22438/jeb/39/1/MRN-662

Guo, H. Q., Wu, H., Yang, N. N., Fu, Q., Liu, F. R., Zhang, H., Hu, R. S., and Hu, Y. F. (2019). "XAS combined with TG–DTG study on synergic effect on sulfur transformation during co-pyrolysis of sawdust and lignite," *Journal of Thermal Analysis and Calorimetry* 135(4), 2475-2480. DOI: 10.1007/s10973-018-7259-y

Han, Z. H., Cao, W. H., Xin-Bao, L. I., and Liu, G. J. (2006). "Analysis of chemical composition of essential oil in *Cornus officinalis* Sieb. et Zucc by GC-MS," *Fine Chemicals* 23(2), 130-129. DOI: 10.1016/S1002-0160(06)60051-9

He, J., Xu, J. K., Pan, X. G., Ye, X. S., Gao, P. Y., Yan, Y., Xu, C. Y., Qiang, G. F., Du, G. H., and Cheng, Y. C. (2019). "Unusual cadinane-type sesquiterpene glycosides with α-glucosidase inhibitory activities from the fruit of *Cornus officinalis* Sieb. et Zucc," *Bioorganic Chemistry* 82, 1-5. DOI: 10.1016/j.bioorg.2018.09.026

Hong, W. U., Liang H., and Liu Y. H. (2003). "Extraction and determination of total saponins from *Cornus officinalis* Sieb. et Zucc," *Journal of the Fourth Military Medical University* 24(5), 430-432. DOI: 10.1023/A:1022080713267

Hu, J. G., Liu Y. L., Song J. Q., and Zhang, L. (2009). "Analysis of aroma components in fruit of *Cornus officinalis* Sieb. et Zucc by GC-MS," *Journal of Northwest A and F University* 194-198.

Hu, S. W., Shima, T., and Hou, Z. M. (2014). "Carbon-carbon bond cleavage and rearrangement of benzene by a trinuclear titanium hydride," *Nature* 512(7515), DOI: 10.1038/nature13624

Jiang, S. C., Ge, S. B., Wu, X., Yang, Y. M., Chen, J. T., and Peng, W. X. (2017). "Treating n-butane by activated carbon and metal oxides," *Toxicological and Environmental Chemistry* 99(5-6), 753-759. DOI: 10.1080/02772248.2017.1279432

Jiang, S. C., Ge, S. B., and Peng, W. X. (2018). "Molecules and functions of rosewood: *Dalbergia stevenson*," *Arabian Journal of Chemistry* 11(6), 782-792. DOI: 10.1016/j.arabjc.2017.12.032.

Kaznowska, E., Depciuch, J., Szmuc, K., and Cebulski, J. (2017). "Use of FTIR spectroscopy and PCA-LDC analysis to identify cancerous lesions within the human colon," *Journal of Pharmaceutical and Biomedical Analysis* 134, 259-268. DOI: 10.1016/j.jpba.2016.11.047

Khan, A. M., Yusoff, I., Abu Bakar, N. K., Abu Bakar, A. F., Alias, Y., and Mispan, M. S. (2018). "Accumulation, uptake and bioavailability of rare earth elements (Rees) in soil grown plants from ex-mining area in Perak, Malaysia," *Applied Ecology and Environmental Research* 15(3), 117-133. DOI: 10.15666/aeer/1503_117133

Koo, B. M., Dalla Corte, D. A., Chazalviel, J. N., Maroun, F., Rosso, M., and Ozanam, F. (2018). "Lithiation mechanism of methylated amorphous silicon unveiled by Operando ATR-FTIR spectroscopy," *Advanced Energy Materials* 8(13), DOI: 10.1002/aenm.201702568

Lan, S. W., and Peng, W.X. (2012). "Py-GC-MS analysis on biomass energy components from wood extractives of *Eucalyptus urophydis* under high temperature," *Applied Mechanics and Materials* 164, 30-32. DOI: 10.4028/www.scientific.net/AMM.164.30

Lanza, I. R., Zhang, S. C., Ward, L. E., Karakelides, H., Raftery, D., and Nair, K. S. (2010). "Quantitative metabolomics by H-NMR and LC-MS/MS confirms altered metabolic pathways in diabetes," *Plos One* 5(5), DOI: 10.1371/journal.pone.0010538

Liu, L. L., Cheng, X. X., Zhao, W. W., Wang, Y. H., Dong, X., Chen, L. L., Zhang, D. Q., and Peng, W. X. (2018). "Systematic characterization of volatile organic components and pyrolyzates from *Camellia oleifera* seed cake for developing high value-added products," *Arabian Journal of Chemistry* 11(6), 802-814. DOI: 10.1016/j.arabjc.2017.12.031

Lou, J. W., Chen, J. T., Ni, C. Y., and Peng, W. X. (2018). "Molecules and functions of rosewood: *Pterocarpus cambodianus*," *Arabian Journal of Chemistry* 11(6), 763-770. DOI: 10.1016/j.arabjc.2017.12.030

Lu, K., Heng, X., Garyu, L., Monti, S., Garcia, E. L., Kharytonchyk, S., Dorjsuren, B., Kulandaivel, G., Jones, S., Hiremath, A., Divakaruni, S. S., LaCotti, C., Barton, S., Tummillo, D., Hosic, A., Edme, K., Albrecht, S., Telesnitsky, A., and Summers, M. F. (2011). "NMR detection of structures in the HIV-1 5'-leader RNA that regulate genome packaging," *Science* 334(6053), 242-245. DOI: 10.1126/science.1210460

Lusk, G., and Gullion, T. (2018). "Description of an RF field-strength controller for solid-state NMR experiments," *Solid State Nuclear Magnetic Resonance* 91, 9-14. DOI: 10.1016/j.ssnmr.2018.01.002

Martin, M., Legat, B., Leenders, J., Vanwinsberghe, J., Rousseau, R., Boulanger, B., Eilers, P. H. C., De Tullio, P., Govaerts, B. (2018). "PepsNMR for ^{1}H NMR metabolomic data pre-processing," *Analytica Chimica Acta* 1019, 1-13. DOI: 10.1016/j.aca.2018.02.067

Maulidiani, M., Mediani, A., Abas, F., Park, Y. S., Park, Y. K., Kim, Y. M., and Gorinstein, S. (2018). "^{1}H NMR and antioxidant profiles of polar and non-polar extracts of persimmon *(Diospyros kaki L.*) - Metabolomics study based on cultivars and origins," *Talanta* 184, 277-286. DOI: 10.1016/j.talanta.2018.02.084

Moniz, P., Serralheiro, C., Matos C. T., Boeriu, C. G., Frissen, A. E., Duarte, L. C., Roseiro, L. B., Pereira, H., and Carvalheiro, F. (2018). "Membrane separation and characterisation of lignin-derived products obtained by a mild ethanol organosolv treatment of rice straw," *Process Biochemistry* 65, 136-145. DOI: 10.1016/j.procbio.2017.11.012

Peng, W. X., Wang, L. S., Lin, Z., and Zheng, Z. Z. (2012). "Py-GC-MS analysis on benzene-alcohol extractives of *Eucalyptus urophydis* wood for fine indoor environment," *Applied Mechanics and Materials* 178-181, 288-291. DOI: 10.4028/www.scientific.net/AMM.178-181.288

Peng, W. X., Xue, Q., and Ohkoshi, M. (2017a). "Immune effects of extractives on bamboo biomass self-plasticization," *Pakistan Journal of Pharmaceutical Sciences* 27(4), 991-999. DOI: 10.4314/tjpr.v13i7.24

Peng, W. X., Li, D. L., Zhang, M. L., Ge, S. B., Mo, B., Li, S. S., and Ohkoshi, M. (2017b). "Characteristics of antibacterial molecular activities in poplar wood extractives," *Saudi Journal of Biological Sciences* 24(2), 399-404. DOI: 10.1016/j.sjbs.2015.10.026

Pinto, J., Oliveira, A. S., Azevedo, J., De Freitas, V., Lopes, P., Roseira, I., Cabral, M., and de Pinho, P. G. (2018). "Assessment of oxidation compounds in oaked Chardonnay wines: A GC-MS and ^{1}H NMR metabolomics approach," *Food Chemistry* 257, 120-127. DOI: 10.1016/j.foodchem.2018.02.156

Renneckar, S., Zink-Sharp, A. G., Ward, T. C., and Glasser, W. G. (2004). "Compositional analysis of thermoplastic wood composites by TGA," *Journal of Applied Polymer Science* 93(3), 1484-1492. DOI: 10.1002/app.20599

Popadyuk, A., Tarnavchyk, I., Popadyuk, N., Kohut, A., Samaryk, V., Voronov, S., and Voronov, A. (2013). "A novel copolymer of n-[(tert-butylperoxy)methyl]acrylamide and maleic anhydride for use as a reactive surfactant in emulsion polymerization," *Reactive & Functional Polymers* 73(9), 1290-1298. DOI: 10.1016/j.reactfunctpolym.2013.07.002.

Rukthong, W., Thanatawee, P., Sunphorka, S., Piumsomboon, P., and Piumsomboon, P. (2015). "Computation of biomass combustion characteristic and kinetic parameters by using thermogravimetric analysis," *Engineering Journal-Thailand* 19(2), 41-57. DOI: 10.4186/ej.2015.19.2.41

Salasinska, K., Gajek, A., M Celiński, Mizera, K., and Duszak, K. (2020). "Thermal stability of epoxy resin modified with developed flame retardant system based on renewable raw materials," *Materials Science Forum* 995, 43-48. DOI: 10.4028/www.scientific.net/MSF.995.43

Sharma, D., and Rajarathnam, K. (2000). "^{13}C NMR chemical shifts can predict disulfide bond formation," *Journal of Biomolecular NMR* 18(2), 165-171. DOI: 10.1023/A:1008398416292

Shenderova, O., Panich, A. M., Moseenkov, S., Hens, S. C., Kuznetsov, V., and Vieth, H. M. (2011). "Hydroxylated detonation nanodiamond: FTIR, XPS, and NMR studies," *Journal of Physical Chemistry C* 115(39), 19005-19011. DOI: 10.1021/jp205389m

Shupe, A. M., Kiemle, D. J., and Liu, S. (2012). "Quantitative 2D HSQC NMR analysis of mixed wood sugars in hemicellulosic hydrolysate fermentation broth," *Journal of Bioprocess Engineering and Biorefinery* 1(1), 93-100. DOI: 10.1166/jbeb.2012.1007

Tan, F., Liu, Q. L., Zhang, Y. J., Yang, L. Z. and Hu, M. (2006). "Effects of Huanshaodan on the activity of GSH - Px and the content of MDA in rat," *Guiding Journal of TCM* 12(7), 12-15. DOI: 10.3969/j.issn.1672-951X.2006.07.001

Tang, R. G., Ding, C. F., Dang, F., Ma, Y. B., Wang, J. S., Zhang, T. L., and Wang, X. X. (2018). "NMR-based metabolic toxicity of low-level Hg exposure to earthworms," *Environmental Pollution* 239, 428-437. DOI: 10.1016/j.envpol.2018.04.027

Toraman, H. E., Abrahamsson, V., Vanholme, R., Van Acker, R., Ronsse, F., Pilate, G., Boerjan, W., Van Geem, and K. M., Marin, G. B. (2017). "Application of Py-GC/MS coupled with PARAFAC2 and PLS-DA to study fast pyrolysis of genetically engineered poplars," *Journal of Analytical and Applied Pyrolysis* 129, 101-111. DOI: 10.1016/j.jaap.2017.11.022

Vassilev, S. V., and Vassileva, C. G. (2016). "Composition, properties and challenges of algae biomass for biofuel application: An overview," *Fuel* 181, 1-33. DOI: 10.1016/j.fuel.2016.04.106

Wan-Ibrahim, W. S., Ismail, T. N. N. T., Mohd-Salleh, S. F., and Ismail, N. (2018). "GC-MS analysis of phytochemical compounds in aqueous leaf extract of *Abrus precatorius*," *Pertanika Journal of Tropical Agricultural Science* 41(1), 241-250.

Wang, Y. G., Li, X. R., Jiang, Q. J., Sun, H. N., Jiang, J. F., Chen, S. M., Guan, Z. Y., Fang, W. M., and Chen, F. D. (2018). "GC-MS analysis of the volatile constituents in the leaves of 14 Compositae plants," *Molecules* 23(1). DOI: 10.3390/molecules23010166

Wu, J. J., Lorenzo, P., Zhong, S. Y., Ali, M., Butts, C. P., Myers, E. L., and Aggarwal, V. K. (2017). "Synergy of synthesis, computation and NMR reveals correct baulamycin structures," *Nature* 547(7664), 436-440. DOI: 10.1038/nature23265

Xiao, X., Wen, J. Y., Wang, Y. Y., Bian, J., Li, M. F., Peng, F., and Sun, R. C. (2018). "NMR and ESI-MS spectrometry characterization of autohydrolysis xylo-oligosaccharides separated by gel permeation chromatography," *Carbohydrate Polymers* 195, 303-310. DOI: 10.1016/j.carbpol.2018.04.088

Xie, C. P., Li, K. F., Li, Y., Lin, J. L., and Xu, K. M. (2011). "Study on volatile substances of different provenances teak (*Tectona grandis* l.f) wood by TGA," *Advanced Materials Research* 295-297, 88-92. DOI: 10.4028/www.scientific.net/AMR.295-297.88

Xie, Y. Z., Ge, S. B., Jiang, S. C., Liu, Z. L., Chen, L., Wang, L. S., Chen, J. T., Qin, L. C., and Peng, W. X. (2017). "Study on biomolecules in extractives of *Camellia oleifera* fruit shell by GC-MS," *Saudi Journal of Biological Sciences* 25(2), 234-236. DOI: 10.1016/j.sjbs.2017.08.006

Xu, G. Q., Wang, L. H., Liu, J. L., and Wu, J. Z. (2013). "FTIR and XPS analysis of the changes in bamboo chemical structure decayed by white-rot and brown-rot fungi," *Applied Surface Science* 280, 799-805. DOI: 10.1016/j.apsusc.2013.05.065

Xue, B. L., Wen, J. L., and Sun R. C. (2014). "Lignin-based rigid polyurethane foam reinforced with pulp fiber: Synthesis and characterization," *ACS Sustainable Chemistry & Engineering* 2(6), 1474-1480. DOI: 10.1021/sc5001226

Yao, L., Yang, H. T., Yoo, C. G., Meng, X. Z., Pu, Y. Q., Hao, N. J., and Ragauskas, A. J. (2018). "Characteristics of lignin fractions from dilute acid pretreated switchgrass and their effect on cellobiohydrolase from *Trichoderma longibrachiatum*," *Frontiers in Energy Research* 6, DOI: 10.3389/fenrg.2018.00001

Yu, Z. S., Dai, M. Q., Huang, M. M., Fang, S. W., Xu, J. C., Lin, Y., and Ma, X. Q. (2018). "Catalytic characteristics of the fast pyrolysis of microalgae over oil shale: Analytical Py-GC/MS study," *Renewable Energy* 125, 465-471. DOI: 10.1016/j.renene.2018.02.136

Zabow, G., Dodd, S. J., and Koretsky, A. P. (2015). "Shape-changing magnetic assemblies as high-sensitivity NMR-readable nanoprobes," *Nature* 520(7545), 73-U157. DOI: 10.1038/nature14294

Zhang, J. Z., Kang, H. J., Gao, Q., Li, J. Z., Pizzi, A., Delmotte, L. (2015). "Performances of larch (*Larix gmelinii*) tannin modified urea-formaldehyde (TUF) resin and plywood bonded by TUF resin," *Journal of Applied Polymer Science* 131(22), 41064. DOI: 10.1002/app.41064

Zhang, Q. C., Zhao, Y., Bian, H. M. (2013). "Antiplatelet activity of a novel formula composed of malic acid, succinic acid and citric acid from *Cornus officinalis* fruit," *Phytotherapy Research* 27(12), 1894-1896. DOI: 10.1002/ptr.4934

Article submitted: June 9, 2022; Peer review completed: July 30, 2022; Revisions accepted: September 23, 2022; Published: September 29, 2022.
DOI: 10.15376/biores.17.4.6411-6444

APPENDIX

(Supplementary Information)

Table S1. GC-MS Analysis of Sample B1

No.	Retention Time (min)	Peak Area (%)	Component
1	5.251	9.21	3-Furaldehyde
2	5.466	4.44	Maleic anhydride
3	6.902	0.19	2-Furancarboxaldehyde, 5-methyl-
4	7.11	0.18	2,4-Dihydroxy-2,5-dimethyl-3(2H)-furan-3-one
5	8.757	0.19	Thymine
6	8.85	0.91	3-Furancarboxylic acid, methyl ester
7	9.378	0.93	Levoglucosenone
8	9.923	1.46	4H-Pyran-4-one, 2,3-dihydro-3,5-dihydroxy-6-methyl-
9	10.276	0.23	Dehydromevalonic lactone
10	10.389	0.30	2-Butenedioic acid, monoethyl ester
11	11.056	0.19	Benzaldehyde, 4-methyl-
12	11.216	0.52	3-Methyl-2-oxo-2H-pyrane-6-carboxylic acid
13	11.475	16.48	5-Hydroxymethylfurfural
14	11.873	0.19	Butanedioic acid, hydroxy-, diethyl ester, (.+/-.)-
15	12.284	2.73	Malic Acid
16	12.488	0.23	Acetic acid, TBDMS derivative
17	12.58	4.35	Malic Acid
18	12.768	0.36	Ethanone, 1-(2-hydroxy-5-methylphenyl)-
19	13.107	0.85	l-Alanine, N-isobutoxycarbonyl-, butyl ester
20	13.611	0.37	Propanoic acid, 3-chloro-, 4-formylphenyl ester
21	13.926	2.93	4-Ethylbiphenyl
22	13.951	0.46	4-Fluorobenzyl alcohol, TBDMS derivative
23	14.01	16.61	1,2,3-Benzenetriol
24	14.257	1.82	Vanillin
25	14.345	0.56	3,5-Dimethyl-1-dimethylphenylsilyloxybenzene
26	15.157	0.25	Phenol, 2-methoxy-4-propyl-
27	15.982	0.18	Benzoic acid, 4-hydroxy-
28	16.145	0.53	Carbamic acid, monoammonium salt
29	16.277	0.17	2-Propanone, 1-(4-hydroxy-3-methoxyphenyl)-
30	16.315	0.22	Tricyclo[3.3.1.1(3,7)]decane-2-ol-1-carboxylic acid, methyl ester
31	16.391	0.21	Homovanillic acid
32	16.836	0.29	3-Hydroxy-4-methoxybenzoic acid
33	17.089	0.31	Butyrovanillone

34	18.025	0.43	Homovanillic acid
35	18.449	0.19	Dodecanoic acid, 1,1-dimethylpropyl ester
36	18.61	2.58	Spiro[4.5]decan-7-one, 1,8-dimethyl-8,9-epoxy-4-isopropyl-
37	18.776	0.25	2-Propenoic acid, 3-(4-methoxyphenyl)-
38	19.16	0.31	2-Propanone, 1-hydroxy-3-(4-hydroxy-3-methoxyphenyl)-
39	21.893	0.66	n-Hexadecanoic acid
40	22.818	0.17	Imidazo[4,5-c]pyridine, 1-benzyl-2-(2-pyridyl)-
41	22.842	0.47	2-(Methylthio)phenazine
42	22.948	0.31	[1,2,3]Triazolo[4,5-e][1,4]diazepine-5,8-dione, 1,4,6,7-tetrahydro-
43	23.47	0.56	12,13-Epoxy-11-hydroxyoctadec-9-enoic acid, methyl ester, trimethylsilyl ether
44	23.575	0.71	6-Thiopyrazolo[3,4-d]pyrimidin-4,6(5H,7H)-dione-3-carboxamide
45	23.652	1.88	Ethylamine, N,N-diheptyl-2-(2-thiophenyl)-
46	23.663	0.55	3-Cyclopentylpropionic acid, 4-biphenyl ester
47	23.806	0.69	Bismuthine, triphenyl-
48	23.846	1.53	1,1'-Biphenyl, 4-butoxy-
49	24.089	2.30	9,12-Octadecadienoic acid (Z,Z)-
50	24.125	0.87	2(3H)-Furanone, dihydro-5-tetradecyl-
51	24.371	0.47	Linoleic acid ethyl ester
52	24.564	0.62	2,8-Disilatricyclo[7.3.0.0(3,7)]dodeca-4,6,10,12-tetraene, 2,2,8,8-tetramethyl-
53	25.205	0.19	Ethanol
54	25.367	0.26	1,1'-Biphenyl, 4-butoxy-
55	25.611	0.22	Tributyl acetylcitrate
56	25.919	0.23	Ethanol
57	26.057	0.23	Thiazolo[4,5-c]pyridin-2-amine, N-phenyl-
58	26.602	0.28	Ethanol
59	27.165	0.47	1-Hexadecanesulfonamide, N-(3-acetylphenyl)-
60	27.182	0.37	13-Docosenoic acid, (Z)-, TBDMS derivative
61	27.271	0.35	Ethanol
62	27.521	0.29	Ethylamine, N,N-diheptyl-2-phenylthio
63	27.812	0.24	2-Chloroaniline-5-sulfonic acid
64	27.921	0.38	Ethanol
65	28.309	0.25	Ethylamine, N,N-diheptyl-2-(2-thiophenyl)-
66	28.433	0.17	Fenoterol, N-trifluoroacetyl-O,O,O,O-tetrakis(trimethylsilyl)deriv.
67	28.549	0.41	Ethanol
68	28.939	0.19	Ethylamine, N,N-diheptyl-2-phenylthio
69	29.119	0.32	2-Chloroaniline-5-sulfonic acid

70	29.142	0.42	Ethanol
71	29.304	0.86	Vitamin E
72	29.539	0.19	L-Alanine, N-[N-[N-[(2-hydroxy-1-naphthalenyl)methylene]-L-valyl]-L-isoleucyl]-, ethyl ester
73	29.726	0.45	1-[2,4-Bis(trimethylsiloxy)phenyl]-2-[(4-trimethylsiloxy)phenyl]propan-1-one
74	29.741	0.42	Ethanol
75	30.301	0.48	Phenol, 2,6-bis(1,1-dimethylethyl)-4-[(4-hydroxy-3,5-dimethylphenyl)methyl]-
76	30.323	0.41	Ethanol
77	30.826	0.32	1-Heptene, 1,3-diphenyl-1-(trimethylsilyloxy)-
78	30.894	0.38	Ethanol
79	31.448	0.35	Ethanol
80	31.968	0.47	4H-1-Benzopyran-4-one, 6,7-dimethoxy-3-phenyl-
81	31.988	0.30	Ethanol
82	32.376	0.17	Carbonic acid, 4-[[(4-methoxyphenyl)methylene]amino]phenyl pentyl ester
83	32.492	1.01	4-Methyl-2,4-bis(p-hydroxyphenyl)pent-1-ene, 2TMS derivative
84	32.514	0.27	Ethanol
85	32.863	0.37	4-Benzoyl-N-(4-methoxy-phenyl)-benzamide
86	32.905	0.20	Phthalic acid, 3,5-dimethylphenyl 4-formylphenyl ester
87	32.993	1.37	Cyclotetrasiloxane, octamethyl-
88	33.035	0.23	Ethanol
89	33.419	0.22	4-Acetylphenyl 5-acetyl-2-methoxyphenyl ether
90	33.506	0.42	4-Benzoyl-N-(4-methoxy-phenyl)-benzamide
91	33.572	1.04	5-Hydroxy-7-methoxy-2-methyl-3-phenyl-4-chromenone
92	33.598	0.22	Ethanol
93	33.686	0.22	4-Methyl-2,4-bis(p-hydroxyphenyl)pent-1-ene, 2TMS derivative

Table S2. GC-MS Analysis of Sample B2

No.	Retention Time (min)	Peak Area (%)	Component
1	5.218	7.29	3-Furaldehyde
2	5.461	5.25	Maleic anhydride
3	6.879	0.33	2-Furancarboxaldehyde, 5-methyl-
4	7.081	0.33	2,4-Dihydroxy-2,5-dimethyl-3(2H)-furan-3-one
5	8.845	1.03	3-Furancarboxylic acid, methyl ester
6	9.156	0.34	Acetic acid, 1-(2-methyltetrazol-5-yl)ethenyl ester
7	9.188	0.38	2-Butenedioic acid (E)-, monomethyl ester
8	9.363	0.52	Levoglucosenone

9	9.931	1.95	4H-Pyran-4-one, 2,3-dihydro-3,5-dihydroxy-6-methyl-
10	11.05	0.25	Benzaldehyde, 4-methyl-
11	11.3	0.66	Malic Acid
12	11.537	17.34	5-Hydroxymethylfurfural
13	11.8	0.76	5-Hydroxymethylfurfural
14	11.917	4.29	Malic Acid
15	12.074	0.62	2-Propoxy-succinic acid, dimethyl ester
16	13.233	0.54	Ethyldiethanolamine, O,O'-diacetyl
17	13.444	0.33	.beta.-Naphthyl myristate
18	13.624	0.27	Propanoic acid, 3-chloro-, 4-formylphenyl ester
19	13.657	0.28	Benzoic acid, 4-formyl-, methyl ester
20	13.919	5.25	4-Ethylbiphenyl
21	14.058	23.46	1,2,3-Benzenetriol
22	14.274	1.25	Vanillin
23	14.353	0.84	3,5-Dimethyl-1-dimethylphenylsilyloxybenzene
24	16.802	0.74	.beta.-D-Glucopyranose, 1,6-anhydro-
25	16.84	0.26	3-Hydroxy-4-methoxybenzoic acid
26	17.104	0.31	Butyrovanillone
27	18.04	0.38	Benzenepropanol, 4-hydroxy-3-methoxy-
28	18.23	0.41	n-Butyric acid 2-ethylhexyl ester
29	18.596	1.58	Spiro[4.5]decan-7-one, 1,8-dimethyl-8,9-epoxy-4-isopropyl-
30	18.772	0.28	2-Propenoic acid, 3-(4-methoxyphenyl)-
31	19.179	0.29	2-Propanone, 1-hydroxy-3-(4-hydroxy-3-methoxyphenyl)-
32	21.163	0.34	Benzo[b]-1,8-naphthyridin-5(10H)-one, 10-methyl-
33	21.898	0.54	n-Hexadecanoic acid
34	22.757	0.53	2-(p-Phenoxyphenyl)indolizine
35	22.885	1.03	1H-Benzo[d,E]phthalazine, 6-methoxy-1,3-dimethyl-
36	23.264	1.45	1H-Benzo[d,E]phthalazine, 6-methoxy-1,3-dimethyl-
37	24.09	2.21	9,12-Octadecadienoic acid (Z,Z)-
38	24.127	0.81	2(3H)-Furanone, dihydro-5-tetradecyl-
39	27.247	0.38	1,3-Benzenediol, o-(4-methylbenzoyl)-o'-(2-methoxybenzoyl)-
40	27.261	0.79	13-Docosenoic acid, (Z)-, TBDMS derivative
41	27.486	0.26	Hydrazinecarboxamide
42	28.121	0.29	Hydrazinecarboxamide
43	28.748	0.30	Hydrazinecarboxamide
44	29.361	0.32	Hydrazinecarboxamide
45	29.928	0.39	4-Methyl-2,4-bis(p-hydroxyphenyl)pent-1-ene, 2TMS derivative
46	29.959	0.31	Hydrazinecarboxamide

47	30.541	0.31	Hydrazinecarboxamide
48	30.916	1.16	6H-Dibenzo[b,d]pyran-6-one, 7,9-dihydroxy-3-methoxy-1-methyl-
49	31.051	0.37	3,4-Dihydroxyphenylglycol, 4TMS derivative
50	31.1	0.26	Hydrazinecarboxamide
51	31.57	0.37	1,3,3-Trimethyl-1-(4'-methoxyphenyl)-6-methoxyindane
52	31.614	1.02	Cyclotrisiloxane, hexamethyl-
53	31.627	0.58	4-Methyl-2,4-bis(p-hydroxyphenyl)pent-1-ene, 2TMS derivative
54	31.647	0.26	Hydrazinecarboxamide
55	32.107	0.41	1-Adamantylamine, N-tert-butyldimethylsilyl-
56	32.16	0.56	Hexestrol, O,O'-di(pentafluoropropionyl)-
57	32.663	0.38	Silane, methylvinyl(pent-2-yloxy)tetradecyloxy-
58	32.687	1.77	4-Methyl-2,4-bis(p-hydroxyphenyl)pent-1-ene, 2TMS derivative
59	33.148	0.30	Methane, tribromofluoro-
60	33.186	1.15	tert-Butyldimethylsilyl 3-methyl-4-((2,2,3,3,3-pentafluoropropanoyl)oxy)benzoate
61	33.236	1.54	4-Methyl-2,4-bis(p-hydroxyphenyl)pent-1-ene, 2TMS derivative
62	33.732	0.29	Methane, tribromofluoro-
63	33.788	0.75	1-Adamantylamine, N-tert-butyldimethylsilyl-
64	33.804	0.53	tert-Butyldimethylsilyl 3-methyl-4-((2,2,3,3,3-pentafluoropropanoyl)oxy)benzoate
65	33.954	0.24	1-Adamantylamine, N-tert-butyldimethylsilyl-

Table S3. GC-MS Analysis of Sample B3

No.	Retention Time (min)	Peak Area (%)	Component
1	5.203	6.88	Furfural
2	5.397	2.37	1H-Imidazole, 1,2-dimethyl-
3	5.908	0.25	Phenethylamine, p,.alpha.-dimethyl-
4	7.034	0.63	Phenethylamine, p,.alpha.-dimethyl-
5	8.159	0.26	(S)-(+)-1-Cyclohexylethylamine
6	8.709	0.33	Cyclohexanamine, N-3-butenyl-N-methyl-
7	8.819	1.05	1H-Imidazole-4-carboxylic acid, methyl ester
8	8.987	0.28	1H-Imidazole-4-carboxylic acid, methyl ester
9	9.175	0.70	(S)-(+)-1-Cyclohexylethylamine
10	9.35	2.00	Levoglucosenone
11	9.874	1.13	4H-Pyran-4-one, 2,3-dihydro-3,5-dihydroxy-6-methyl-
12	10.275	0.26	Meso-1,2,3,4-butanetetracarboxylic acid
13	11.032	0.60	N-Chloroacetyl-3,6,9,12-tetraoxapentadec-14-yn-1-amine
14	11.329	18.00	5-Hydroxymethylfurfural

15	12.164	3.92	Malic Acid
16	12.384	1.46	1,2-Cyclobutanedicarboxylic acid, trans-
17	12.552	0.70	1,2-Cyclobutanedicarboxylic acid, trans-
18	12.772	0.70	Melezitose
19	13.561	0.29	5-tert-Butylpyrogallol
20	13.917	10.13	1,2,3-Benzenetriol
21	14.208	3.31	Benzaldehyde, 3-hydroxy-4-methoxy-
22	14.324	1.97	2-(4'-Methoxymethylbiphenyl-4-yl)propan-2-ol
23	15.023	0.20	1-Cyclohexen-3-one, 2-acetyl-1-hydroxy-5,5-dimethyl-
24	15.12	0.32	2,5-Cyclohexadiene-1,4-dione, 2,3-dimethoxy-5-methyl-
25	15.883	0.31	5-tert-Butylpyrogallol
26	16.122	0.27	1-Cyclohexen-3-one, 2-acetyl-1-hydroxy-5,5-dimethyl-
27	16.239	0.27	4-Aminobutyramide, N-methyl-N-[4-(1-pyrrolidinyl)-2-butynyl]-N',N'-bis(trifluoroacetyl)-
28	16.284	0.22	4-Aminobutyramide, N-methyl-N-[4-(1-pyrrolidinyl)-2-butynyl]-N',N'-bis(trifluoroacetyl)-
29	17.073	0.50	3-Isopropoxy-4-methoxybenzamide
30	17.972	0.91	N-2,4-Dnp-L-arginine
31	18.141	0.37	2,4,6-Trimethoxyamphetamine
32	18.587	5.34	2-Acetoxy-3,3-dimethyl-2-(3-oxo-but-1-enyl)-cyclobutanecarboxylic acid, methyl ester
33	19.117	0.56	(E)-4-Hexenoic acid, 2-acetyl-2-(1-buten-3-yl)-, ethyl ester
34	20.224	0.25	N-2,4-Dnp-L-arginine
35	20.359	0.25	1b,4a-Epoxy-2H-cyclopenta[3,4]cyclopropa[8,9]cycloundec[1,2-b]oxiren-5(6H)-one, 7-(acetyloxy)decahydro-2,9,10-trihydroxy-3,6,8,8,10a-pentamethyl-
36	21.873	2.30	N-2,4-Dnp-L-arginine
37	22.054	1.34	Di-sec-butyl phthalate
38	22.436	0.26	Androst-4-en-11-ol-3,17-dione, 9-thiocyanato-
39	23.244	0.22	2,5-Dimethoxy-4-ethylthio-benzaldehyde
40	23.652	1.87	3,4-Dimethoxyphenol, TMS derivative
41	24.021	2.34	9,12-Octadecadienoic acid (Z,Z)-
42	24.085	9.58	9,12-Octadecadienoic acid (Z,Z)-
43	24.331	0.42	2,5-Dimethoxy-4-ethylthio-benzaldehyde
44	24.364	0.60	2,5-Dimethoxy-4-ethylthio-benzaldehyde
45	24.609	0.43	2,5-Dimethoxy-4-ethylthio-benzaldehyde
46	25.082	0.20	2,5-Dimethoxy-4-ethylthio-benzaldehyde
47	26.518	0.81	Androst-4-en-11-ol-3,17-dione, 9-thiocyanato-
48	26.873	0.24	1,2-Cinnolinedicarboxylic acid, 1,2,3,5,6,7,8,8a-octahydro-4-trimethylsilyloxy-, diethyl ester

49	27.275	0.18	Ethanol
50	27.514	0.37	1,2-Cinnolinedicarboxylic acid, 1,2,3,5,6,7,8,8a-octahydro-4-trimethylsilyloxy-, diethyl ester
51	28.141	0.55	1,2-Cinnolinedicarboxylic acid, 1,2,3,5,6,7,8,8a-octahydro-4-trimethylsilyloxy-, diethyl ester
52	28.413	0.19	Ethanol
53	28.769	0.87	Ethanol
54	29.247	1.55	Vitamin E
55	29.357	0.58	Ethanol
56	29.933	0.75	1,2-Cinnolinedicarboxylic acid, 1,2,3,5,6,7,8,8a-octahydro-4-trimethylsilyloxy-, diethyl ester
57	30.211	6.55	Heptasiloxane, 1,1,3,3,5,5,7,7,9,9,11,11,13,13-tetradecamethyl-
58	31.052	0.50	Octasiloxane, 1,1,3,3,5,5,7,7,9,9,11,11,13,13,15,15-hexadecamethyl-
59	31.13	0.31	Heptasiloxane, 1,1,3,3,5,5,7,7,9,9,11,11,13,13-tetradecamethyl-

Table S4. GC-MS Analysis of Sample B4

No.	Retention Time (min)	Peak Area (%)	Component
1	5.242	6.16	Furfural
2	5.449	7.45	Maleic anhydride
3	6.924	0.33	Pyrazole-4-carboxaldehyde, 1-methyl-
4	8.224	0.36	Imidazole, 2-amino-5-[(2-carboxy)vinyl]-
5	8.761	0.42	Cyclohexanamine, N-3-butenyl-N-methyl-
6	8.858	1.26	1H-Imidazole-4-carboxylic acid, methyl ester
7	9.162	0.69	2,3-Dimethylfumaric acid
8	9.382	1.31	Levoglucosenone
9	9.919	1.44	4H-Pyran-4-one, 2,3-dihydro-3,5-dihydroxy-6-methyl-
10	11.058	0.34	Benzene, 1-ethynyl-4-fluoro-
11	11.142	0.55	3-Hydroxydecanoic acid
12	11.439	18.87	5-Hydroxymethylfurfural
13	11.62	1.66	Thiophene, 2-propyl-
14	12.08	0.38	Melezitose
15	12.422	1.07	3-Hydroxydecanoic acid
16	13.024	0.77	2(3H)-Furanone, dihydro-3-(thioacetyl)-
17	13.593	0.35	5-tert-Butylpyrogallol
18	13.989	26.16	1,2,3-Benzenetriol
19	14.253	2.98	1,2,3-Benzenetriol
20	14.35	3.49	1,2,3-Benzenetriol
21	14.596	0.33	Phenol, 2-[(1-methylpropyl)thio]-
22	15.159	0.29	2,5-Cyclohexadiene-1,4-dione, 2,3-dimethoxy-5-methyl-

23	16.802	1.02	6-Thioguanosine
24	17.099	0.43	4-Mercaptobenzoic acid, S-methyl-, methyl ester
25	18.011	0.83	Acetamide, N-Methyl-N-[4-(3-hydroxypyrrolidinyl)-2-butynyl]-
26	18.173	0.87	2-Myristynoyl pantetheine
27	18.613	2.39	2-Acetoxy-3,3-dimethyl-2-(3-oxo-but-1-enyl)-cyclobutanecarboxylic acid, methyl ester
28	19.156	0.40	1-Propyl-3,6-diazahomoadamantan-9-ol
29	21.899	0.87	.alpha.-D-Glucopyranoside, methyl 2-(acetylamino)-2-deoxy-3-O-(trimethylsilyl)-, cyclic methylboronate
30	22.08	0.30	1,2-Benzenedicarboxylic acid, butyl octyl ester
31	22.514	0.42	Androst-4-en-11-ol-3,17-dione, 9-thiocyanato-
32	22.759	0.86	2,5-Dimethoxy-4-ethylthio-benzaldehyde
33	23.568	4.97	2,5-Dimethoxy-4-ethylthio-benzaldehyde
34	23.646	0.59	2,5-Dimethoxy-4-ethylthio-benzaldehyde
35	24.092	3.06	9,12-Octadecadienoic acid (Z,Z)-
36	27.035	0.43	4H-Cyclopropa[5',6']benz[1',2':7,8]azuleno[5,6-b]oxiren-4-one, 8-(acetyloxy)-1,1a,1b,1c,2a,3,3a,6a,6b,7,8,8a-dodecahydro-3a,6b,8a-trihydroxy-2a-(hydroxymethyl)-1,1,5,7-tetramethyl-, (1a.alpha.,1b.beta.,1c.beta.,2a.beta.,3a.beta.,6a.alpha.,6b.alpha.,7.alpha.,8.beta.,8a.alpha.)-
37	29.377	0.48	4H-Cyclopropa[5',6']benz[1',2':7,8]azuleno[5,6-b]oxiren-4-one, 8-(acetyloxy)-1,1a,1b,1c,2a,3,3a,6a,6b,7,8,8a-dodecahydro-3a,6b,8a-trihydroxy-2a-(hydroxymethyl)-1,1,5,7-tetramethyl-, (1a.alpha.,1b.beta.,1c.beta.,2a.beta.,3a.beta.,6a.alpha.,6b.alpha.,7.alpha.,8.beta.,8a.alpha.)-
38	30.929	0.86	Acetic acid, 2,3-dihydro-7-methyl-2-oxo-6-(phenylmethyl)thiazolo[4,5-b]pyridin-5-yl ester
39	31.382	4.54	Octasiloxane, 1,1,3,3,5,5,7,7,9,9,11,11,13,13,15,15-hexadecamethyl-

Table S5. Py-GC-MS Analysis of CON

No.	Retention Time (min)	Peak Area (%)	Component
1	3.70	0.01	Actinobolin
2	4.10	2.82	4-methyl-2-Hexanamine
3	4.26	1.33	Glycidol
4	4.38	0.83	N,N-difluoro-Ethanamine
5	4.74	0.92	Furan
6	4.93	0.03	Ethanethiol
7	4.99	0.15	Methyl glyoxal
8	5.06	1.13	Formic acid

9	5.49	0.26	2,3-Butanedione
10	5.56	0.30	1-Propanol
11	5.70	0.84	3-methyl-Furan
12	5.85	0.21	Acetic acid
13	6.68	8.72	Acetic acid
14	6.87	0.12	3-methyl-3-Buten-2-one
15	6.95	0.61	1-hydroxy-2-Propanone
16	7.15	0.21	Methyl formate
17	7.25	0.12	N-(4-amino-3-furazanyl)-Acetamide
18	7.36	0.07	O-(3-methylbutyl)-Hydroxylamine
19	7.39	0.08	2-methylpropyl ester Formic acid
20	7.55	0.37	2,5-dimethyl-Furan
21	7.68	0.05	Formic acid, 2-methylpropyl ester
22	7.75	0.08	Ethyl formate
23	7.95	0.20	2-Vinylfuran
24	8.10	0.20	Propanoic acid
25	8.23	0.11	2-Propenoic acid
26	8.39	0.13	1H-Pyrrole, 1-methyl-
27	8.65	0.09	Ethanone, 1-(methylenecyclopropyl)-
28	8.80	0.27	2-propenyl ester 2-Propenoic acid
29	8.90	0.03	1,5-Pentanediol
30	8.99	0.03	Propanoic acid, 3-hydroxy-, hydrazide
31	9.13	0.19	Toluene
32	9.24	0.71	Acetic acid, methyl ester
33	9.41	0.07	Acetic acid, hydrazide
34	9.48	0.04	Propanoic acid, 2-methyl-
35	9.58	0.29	Propanal
36	9.83	0.62	Propanoic acid, 2-oxo-, methyl ester
37	10.03	0.22	Glycidol
38	10.13	0.50	3-Amino-s-triazole
39	10.30	0.06	Butanoic acid
40	10.43	0.13	Furfural
41	10.60	0.03	1,6:2,3-Dianhydro-4-O-acetyl-.beta.-d-allopyranose
42	10.64	0.04	2(5H)-Furanone, 3-methyl-
43	10.75	0.04	3-Cyclohepten-1-one
44	10.90	0.15	2-Amino-2-methyl-1,3-propanediol
45	11.16	2.78	Furfural
46	11.21	0.12	2-Cyclopenten-1-one
47	11.33	0.03	Pentane, 1-nitro-
48	11.39	0.04	Propanoic acid, 2-methyl-

49	11.50	0.03	Ethanol, 2-(2-propenyloxy)-
50	11.68	0.11	Maleic anhydride
51	11.83	0.16	Maleic anhydride
52	11.89	0.74	2-Furanmethanol
53	12.00	0.06	Ethylbenzene
54	12.07	0.07	Formaldehyde, methyl(2-propynyl)hydrazone
55	12.21	0.22	1,2-Ethanediol, diacetate
56	12.28	0.05	1,2-Cyclopentanedione
57	12.41	0.01	1-Methyl pyrrolidin-3-amine
58	12.56	0.02	4-Cyclopentene-1,3-dione
59	12.64	0.01	1,4-Cyclohexanediol, trans-
60	12.68	0.00	Acetic acid, 1,4-pentadien-3-yl ester
61	12.74	0.06	2-Pentene, (E)-
62	12.79	0.14	3-Butene-1,2-diol
63	12.96	0.05	Bicyclo[4.2.0]octa-1,3,5-triene
64	13.08	0.12	s-Triazole, 3-acetamido-
65	13.37	0.12	2H-Pyran-2-one, 5,6-dihydro-
66	13.40	0.09	Methacrylic anhydride
67	13.51	0.08	2-Cyclopenten-1-one, 2-methyl-
68	13.64	0.10	Ethanone, 1-(2-furanyl)-
69	13.88	0.40	2(5H)-Furanone
70	14.01	0.14	Methyl propionate
71	14.31	1.06	1,2-Cyclopentanedione
72	14.40	0.04	Butanoic acid, 4-hydroxy-2-methylene-
73	14.55	0.02	Dihydroxyacetone
74	14.62	0.04	2(5H)-Furanone, 5-methyl-
75	14.69	0.11	2,5-Furandione, dihydro-3-methylene-
76	14.87	0.04	Selenium(IV) oxide
77	14.95	0.01	6-Isopropoxytetrazolo[1,5-b]pyridazine
78	15.04	0.06	Benzene, propyl-
79	15.25	0.19	2,3-Pentanedione
80	15.39	0.74	2-Furancarboxaldehyde, 5-methyl-
81	15.50	0.19	Pentanoic acid, 1-cyclopentylethyl ester
82	15.75	0.05	Ethyl acetoacetate
83	15.91	0.49	Phenol
84	16.14	0.03	3-Hexenoic acid, (E)-
85	16.28	0.02	2-Furanmethanol, acetate
86	16.41	0.05	Heptanoic acid
87	16.70	1.02	Oxazolidine, 2,2-diethyl-3-methyl-
88	16.80	1.07	2-Methyliminoperhydro-1,3-oxazine

89	16.88	0.06	3-Cyclobutene-1,2-dione, 3,4-dihydroxy-
90	17.07	0.03	1H-Pyrrole-2-carboxaldehyde
91	17.17	0.04	1H-Pyrrole-2-carboxaldehyde
92	17.29	0.08	4(1H)-Pyrimidinone, 6-hydroxy-
93	17.35	0.08	6-Azacytosine
94	17.51	0.02	Limonene
95	17.72	0.40	1,2-Cyclopentanedione, 3-methyl-
96	17.78	0.04	2-Cyclopenten-1-one, 3,5,5-trimethyl-
97	17.86	0.06	2,5-Furandione, 3,4-dimethyl-
98	17.93	0.05	2-Cyclopenten-1-one, 2,3-dimethyl-
99	18.04	0.18	Benzene, (methoxymethyl)-
100	18.19	0.14	4-Methyl-5H-furan-2-one
101	18.32	0.11	Phenol, 2-methyl-
102	18.39	0.13	Benzene, n-butyl-
103	18.54	0.12	2-Hexanone, 4-methyl-
104	18.60	0.15	Oxalic acid, diisohexyl ester
105	18.77	0.39	(S)-(+)-2',3'-Dideoxyribonolactone
106	18.95	0.41	p-Cresol
107	19.11	0.23	2,5-Furandicarboxaldehyde
108	19.24	0.15	Pyrazine, 2-methoxy-3-methyl-
109	19.50	2.21	Phenol, 2-methoxy-
110	19.59	0.06	Cyclopentanecarboxaldehyde, 2-methyl-3-methylene-
111	19.66	0.03	Cyclopentaneacetaldehyde, 2-formyl-3-methyl-.alpha.-methylene-
112	19.73	0.08	Piperazine, 2-methyl-
113	19.79	0.11	Tert.-butylaminoacrylonitryl
114	19.84	0.27	Pyrimidine-4,6-diol, 5-methyl-
115	19.99	0.09	Benzofuran, 2-methyl-
116	20.12	0.32	2,3-Pentadiene
117	20.27	0.24	Maltol
118	20.34	0.11	2-Cyclopenten-1-one, 3-ethyl-2-hydroxy-
119	20.45	0.11	Isobutyl 2-methylpentyl carbonate
120	20.53	0.11	2H-Pyran-3(4H)-one, dihydro-6-methyl-
121	20.76	0.14	2(1H)-Pyridinone
122	20.85	0.12	3-Pyridinol
123	20.90	0.15	2,3-dimethyl-Phenol
124	21.16	0.47	pentyl-Benzene,
125	21.26	0.05	2,5-Cyclohexadiene-1,4-dione, 2,5-dimethyl-
126	21.35	0.07	3-ethyl-Phenol
127	21.40	0.13	2,3-dimethyl-Phenol

128	21.47	0.12	2,3-Dihydroxybenzaldehyde
129	21.64	0.15	Hydrazine, 1-methyl-1-phenyl-
130	21.70	0.19	2-Methoxy-6-methylphenol
131	21.89	0.15	Methanesulfonamide, N,N-dimethyl-
132	22.08	1.95	Creosol
133	22.28	1.67	Catechol
134	22.52	0.34	2,3-dihydro-Benzofuran
135	22.73	0.44	6,8-Dioxabicyclo[3.2.1]octane, 7-ethyl-5-methyl-, (1R-exo)-
136	22.92	0.37	1-(1H-Imidazol-2-yl)-2,2-dimethyl-propan-1-one
137	23.15	2.07	5-Hydroxymethylfurfural
138	23.39	0.32	E-8-Methyl-7-dodecen-1-ol acetate
139	23.51	1.05	Oxalic acid, monoamide, n-propyl, nonyl ester
140	23.66	0.76	1,2-Benzenediol, 3-methoxy-
141	23.83	0.90	Phenol, 4-ethyl-2-methoxy-
142	23.87	0.13	Ethanone, 1-(2,5-dihydroxyphenyl)-
143	24.00	0.24	2-Hydroxy-5-imidazolic acid, ethyl ester
144	24.15	0.77	1,2-Benzenediol, 4-methyl-
145	24.35	1.03	Ethanone, 1-(5-ethyl-1,3-dioxan-5-yl)-
146	24.52	2.55	2-Methoxy-4-vinylphenol
147	24.60	0.43	1-Butoxypropan-2-yl 2-methylbutanoate
148	24.71	0.33	Thiophene, 2-formyl-2,3-dihydro-
149	24.79	0.16	2H-Imidazole-2-thione, 1,3-dihydro-1-methyl-
150	24.83	0.13	Heptyl S-2-(diisopropylamino)ethyl isopropylphosphonothiolate
151	24.89	0.46	2-Imidazolidinone, 1,3-dimethyl-
152	24.98	0.18	1H-1,2,4-Triazole-3-methanol, 5-amino-
153	25.14	1.87	Phenol, 2,6-dimethoxy-
154	25.21	0.64	Phenol, 2-methoxy-3-(2-propenyl)-
155	25.36	0.64	Phenol, 2-methoxy-4-propyl-
156	25.46	0.10	Butanedioic acid, methyl-
157	25.54	0.24	Methyl 4,6-decadienyl ether
158	25.67	0.50	4-Ethylthiophenol
159	25.90	1.29	1,2,3-Benzenetriol
160	26.02	1.81	Vanillin
161	26.22	0.62	2H-Pyran-2-one, 4-hydroxy-6-(2-oxopropyl)-
162	26.37	0.19	Pyrazole-5-carboxylic acid, 3-methyl-
163	26.41	0.13	Pyrazole-5-carboxylic acid, 3-methyl-
164	26.45	0.29	1,2,3-Benzenetriol
165	26.64	1.55	3,5-Dimethoxy-4-hydroxytoluene
166	26.70	1.52	trans-Isoeugenol

167	26.91	0.68	Phenol, 2-methoxy-4-propyl-
168	27.01	0.11	4(1H)-Isobenzofuranone, hexahydro-3a,7a-dimethyl-, cis-(.+/-.)-
169	27.07	0.21	4-Hydroxyimino-4,5,6,7-tetrahydrobenzofurazan
170	27.18	0.20	Pentadecane
171	27.22	0.18	Benzene, hexamethyl-
172	27.38	0.59	Apocynin
173	27.48	0.25	3-Amino-4-methoxybenzamide
174	27.59	0.08	Formamide, N-(3-methyl-5-isoxazolyl)-
175	27.66	0.24	3-Ethoxy-4-methoxybenzaldehyde
176	27.77	0.18	Benzoic acid, 4-hydroxy-3-methoxy-, methyl ester
177	27.85	0.59	Hydroquinone, TMS derivative
178	27.93	0.18	3,4-Altrosan
179	28.08	1.11	2-Propanone, 1-(4-hydroxy-3-methoxyphenyl)-
180	28.23	0.86	.beta.-D-Glucopyranose, 1,6-anhydro-
181	28.55	3.27	(E)-Stilbene
182	28.63	0.91	.beta.-D-Glucopyranose, 1,6-anhydro-
183	28.81	1.95	D-Allose
184	28.94	1.54	.beta.-D-Glucopyranose, 1,6-anhydro-
185	29.01	1.14	D-Allose
186	29.09	0.50	D-Allose
187	29.17	1.67	.beta.-D-Glucopyranose, 1,6-anhydro-
188	29.28	0.24	4-Propyl-1,1'-diphenyl
189	29.43	0.63	2-Dodecenoic acid
190	29.70	0.17	Octadecanoic acid
191	29.82	0.18	Eicosanoic acid
192	29.85	0.20	Tricyclo[3.3.1.1(3,7)]decane-2,6-dione, 4-hydroxy-
193	30.02	0.16	dl-Serine, N-acetyl-, methyl ester, acetate (ester)
194	30.11	0.27	(E)-2,6-Dimethoxy-4-(prop-1-en-1-yl)phenol
195	30.24	0.74	Benzenepropanol, 4-hydroxy-3-methoxy-
196	30.36	0.29	3-Heptadecene, (Z)-
197	30.44	0.54	Benzaldehyde, 4-hydroxy-3,5-dimethoxy-
198	30.61	0.10	1,5,9-Decatriene, 2,3,5,8-tetramethyl-
199	30.70	0.20	2-Naphthalenol, 3-methoxy-
200	30.75	0.16	Tetradecane, 4-methyl-
201	30.79	0.20	1-Oxa-4-thiaspiro[4.4]nonane
202	30.90	0.24	4-Methoxymethyl-6-methyl-1H-pyrazolo[3,4-b]pyridin-3-ylamine
203	31.06	0.22	4,7-Dimethoxyindan-1-one
204	31.21	1.12	(E)-2,6-Dimethoxy-4-(prop-1-en-1-yl)phenol
205	31.33	0.25	2-Mercaptobenzothiazole

206	31.49	0.18	Phenazine, 5,10-dihydro-1,3-dinitro-
207	31.76	0.29	4(3H)-Pteridinone, 3-hydroxy-7-methyl-
208	32.09	0.51	Ethanone, 1-(4-hydroxy-3,5-dimethoxyphenyl)-
209	32.19	0.21	Tetradecanoic acid
210	32.28	0.21	Phenol, 4-(ethoxymethyl)-2-methoxy-
211	32.43	0.15	4-Sec-butyl-5-methyl-2-phenyl-4,5-dihydrooxazole-4-carboxylic acid, methyl ester
212	32.74	0.35	7-Pentadecyne
213	33.02	0.65	2-Pentanone, 1-(2,4,6-trihydroxyphenyl)
214	33.38	0.59	1,4-Benzenedimethanol, .alpha.,.alpha.'-bis(azidomethyl)-
215	33.76	0.16	Citronellol
216	34.24	0.11	(1S,15S)-Bicyclo[13.1.0]hexadecan-2-one
217	34.35	0.08	13-Oxabicyclo[9.3.1]pentadecane
218	34.54	0.24	2-Azafluorenone
219	34.62	0.13	Benzoic acid, 2-fluoro-4,5-dimethoxy-
220	34.75	0.13	Benzenemethanol, 3,4,5-trimethoxy-
221	34.94	0.14	8-Phenyloctanoic acid
222	35.44	0.35	Octadecanoic acid
223	35.59	0.30	Octadecanoic acid
224	35.76	0.18	2H-1,3-Oxazine, 2-[(2,6-dimethylphenyl)imino]tetrahydro-
225	36.37	0.12	Neric acid
226	36.45	0.04	Oleic Acid
227	36.98	0.45	5-(3-Hydroxypropyl)-2,3-dimethoxyphenol
228	37.58	0.04	Methyl 18-fluoro-octadecanoate
229	37.79	0.03	(E)-15,16-Dinorlabda-8(17),12-dien-14-al
230	37.88	0.02	(E)-15,16-Dinorlabda-8(17),12-dien-14-al
231	37.99	0.03	3a,9-Dimethyldodecahydrocyclohepta[d]inden-3-one
232	38.21	0.03	9-Hexadecenoic acid
233	38.36	0.05	6-Amino-2,4-dimethyl-8-methoxyquinoline
234	38.47	0.04	Oleic Acid
235	38.95	0.04	Palmitoleic acid
236	39.39	1.31	n-Hexadecanoic acid
237	39.67	0.04	Diazene, 1-(4-methylphenyl)-2-(trimethylsilyl)-
238	39.71	0.01	Octadecanoic acid
239	39.75	0.05	Tridecanoic acid
240	40.17	0.03	Pyrene, hexadecahydro-
241	40.71	0.02	1-Eicosene